



universität
wien



Yale University
School of Medicine



Marshallplan-Jubiläumsstiftung
Austrian Marshall Plan Foundation

Fostering Transatlantic Excellence

Investigation of inflammasome activation and relation to serine proteases

submitted by

Lena Artner, MSc

Vienna 2018

Host Institution

Supervisor at host university:

Yale School of Medicine

Richard A. Flavell

Home University:

Supervisor at home University:

University of Vienna

Thomas Decker

Acknowledgements

First of all, I want to thank Richard A. Flavell for the grand opportunity to work in his Laboratory at the Yale School of Medicine, with and alongside some of the greatest minds in science, teaching me how to conduct truly innovative research and my alma mater, the University of Vienna, including my supervisor Thomas Decker, for building the foundation of this thesis and my future scientific career. In addition, I want to thank the Marshal Plan Foundation for granting me their generous scholarship which funded my Master Thesis work and therefore made my studies possible.

I was pleased to join this genuinely vivid and scientifically stimulating environment, making my stay to one of the most impressionable experiences. I want to sincerely thank all Flavallians, for the great working environment, their intriguing scientific discussions, and the great fun we shared in and outside the Lab. I specifically want to thank Ricky, for being my mentor, a great supervisor and fantastic colleague and friend. He gave his best to give me insights in as many techniques as he knew and it was great fun to learn some of the techniques we both never did before together. Not only did I learn technical skills which will provide the base of my future scientific work but more importantly he encouraged and sharpened my critical thinking and showed me how to deal with the ups and downs that come along with the job we are choosing. Thank you for being critical and detail oriented, and expecting a lot from my end.

Working together not only expanded my methodological skill set but also taught me the kind of creativity and critical thinking required for truly innovative research. I was repeatedly amazed by the Flavallien's way of collaborative and interdisciplinary work and constructive exchange of expertise and ideas and will carry on this way of performing science throughout my future career.

My whole-hearted gratitude goes to my dearest friends and family; it is because of you and your support throughout my whole life that I am now able to present this work.

Last, but everything but least, my deepest appreciations to my best friend, partner and love Sascha, for his great support throughout every day we have had the joy to know each other.

You made it possible for me to reach for my goals and accomplish them, thank you all for this.

Table of Contents

| | |
|---|-----------|
| ACKNOWLEDGEMENTS | 2 |
| LIST OF ABBREVIATIONS | 5 |
| ABSTRACT | 8 |
| INTRODUCTION | 9 |
| THE IMMUNITY OF CANCER..... | 9 |
| <i>Anti-tumor response</i> | 10 |
| <i>Pro-tumorigenic environment</i> | 11 |
| <i>Immunotherapy as cancer treatment</i> | 12 |
| THE DUAL ROLE OF INFLAMMATION IN TUMOR PROGRESSION AND SURVEILLANCE..... | 13 |
| INFLAMMASOMES: INTRACELLULAR SENSOR PLATFORMS DRIVING INFLAMMATION..... | 14 |
| <i>The NLRP1 inflammasome and its role in autoinflammation</i> | 15 |
| <i>Inflammasomes as targets in cancer-immunotherapy</i> | 17 |
| DIPEPTIDYL PEPTIDASES, A DIVERSE PROTEASE FAMILY INVOLVED IN INFLAMMATION, METABOLISM AND HOMEOSTASIS..... | 17 |
| <i>DPP4 family members: DPP8, DPP9 and FAP</i> | 18 |
| <i>Inhibitors of Dipeptidyl Peptidases</i> | 19 |
| <i>Valboro-Pro</i> | 20 |
| SERINE PROTEASES AS INFLAMMASOME MODULATORS | 21 |
| MATERIALS AND METHODS | 25 |
| MOUSE MODELS..... | 25 |
| CELL LINES | 25 |
| REAGENTS..... | 25 |
| TUMOR MODELS..... | 26 |
| GENERATION OF MOUSE BONE MARROW DERIVED MACROPHAGES | 26 |
| CYTOKINE DETECTION WITH ELISA | 26 |
| GENERATION OF THP1 KO CELL LINES FOR DPPs AND INFLAMMASOME COMPONENTS..... | 27 |
| <i>lentiCRISPRv2 single guide targeting</i> | 28 |
| <i>lentiCRISPRv2 two guide strategy</i> | 29 |
| VIRUS GENERATION FOR CRISPR/CAS9 TARGETING AND TRANSDUCTION IN THP1 CELLS | 30 |
| <i>Virus generation in HEK293 FS* cells</i> | 30 |
| <i>Lentiviral transduction in THP1 cells</i> | 30 |

| | |
|---|-----------|
| DNA ISOLATION | 31 |
| LDH RELEASE ASSAY | 31 |
| PROTEIN ISOLATION | 32 |
| SDS POLYACRYLAMIDE GEL ELECTROPHORESIS AND WESTERN BLOT ANALYSIS | 32 |
| DPP ACTIVITY ASSAY | 33 |
| SPECK FORMATION MICROSCOPY | 34 |
| STATISTICAL ANALYSIS | 34 |
| RESULTS AND DISCUSSION | 35 |
| NLRP1 IS THE RESPONSIVE SENSOR FOR VALBORO-PRO INDUCED PYROPTOSIS IN MBMDMS | 35 |
| VALBORO-PRO DOES NOT ALTER TUMOR GROWTH IN EL4 CANCER MODELS..... | 39 |
| VBP MEDIATES TUMOR GROWTH SUPPRESSION IN SYNGENEIC MC38 AND YUMMER1.7 CANCER MODELS | 42 |
| VALBORO-PRO INDUCED PYROPTOSIS IN THP1 CELLS IS DEPENDENT ON CASPASE1..... | 45 |
| VALBORO-PRO AND CHANGES IN REDOX POTENTIAL INHIBIT DPP ACTIVITY IN VITRO..... | 48 |
| SUMMARY | 52 |
| OUTLOOK AND FUTURE PROSPECTIVE | 53 |
| SUPPLEMENTARY FIGURES | 56 |
| LIST OF FIGURES | 57 |
| LIST OF TABLES | 58 |
| REFERENCES | 59 |

List of Abbreviations

| | |
|---------------|---|
| AIM2 | absent in melanoma 2 |
| Ala | alanine |
| AOM-DSS | azoxymethane-dextran sulfate sodium |
| APC | antigen presenting cell |
| ASC | apoptosis-associated speck like protein containing a CARD |
| Asp | aspartic acid |
| B cells | bursa dependent lymphocytes |
| CAF | cancer associated fibroblast |
| CANTOS | canakinumab anti-inflammatory thrombosis outcome study |
| CARD | caspase activation and recruitment domain |
| Casp1 | caspase-1 |
| CRISPR | Clustered Regularly Interspaced Short Palindromic Repeats |
| CTL | cytotoxic T cells |
| CTLA4 | cytotoxic T-lymphocyte associated antigen 4 |
| CXCL | C-X-C chemokine motive ligand |
| DAMP | danger associated molecular pattern |
| DAPI | 4',6-diamidino-2-phenylindole |
| DC | dendritic cells |
| DMEM | Dulbecco's Modified Eagle Medium |
| DMSO | dimethyl sulfoxide |
| DNA | deoxyribonucleic acid |
| DPBS | Dulbecco's phosphate buffered saline |
| DPP | dipeptidyl peptidase |
| ECM | extracellular matrix |
| EDTA | ethylenediaminetetraacetic acid |
| ENU | N-ethyl-N- nitrosourea |
| FAP | fibroblast activating protein |
| FBS | fetal bovine serum |
| FGF2 | fibroblast growth factor 2 |
| FIIND | function to find domain |
| FKLC | familial keratosis lichenoides chronica |
| FlaA | flagellin of Legionella pneumophila |
| GFP | green fluorescent protein |
| GLP-1 | glucagon-like peptide 1 |
| Glut | glutamine |
| GOI | gene of interest |
| GOF | gain of function |
| GSDMD | gasdermin D |
| H-Gly-Pro-pNA | H-Gly-Pro-p-nitroanilide |
| HAMP | homeostasis altering molecular pathway |
| HEPES | N-2-hydroxyethylpiperazine-N-2-ethane sulfonic acid |
| His | histidine |
| HLA | human leucozyte antigen |
| HRP | horserradish peroxidase |
| IFN | interferon |

| | |
|----------|---|
| IL | interleukin |
| LDH | lactate dehydrogenase |
| LF | lethal factor |
| LPS | lipopolysaccharide |
| LRR | leucine rich repeats |
| M-CSF | macrophage colony stimulating factor |
| mBMDM | mouse bone marrow derived macrophage |
| MetOH | methanol |
| MHC | major histocompatibility complex |
| MSPC | multiple self-healing palmoplantar carcinoma |
| NEU | N-ethyl-N- nitrosourea |
| NHEJ | non-homologous end joining |
| NK | natural killer cells |
| NLR | NOD-like receptor |
| NLRC | NOD-, LRR- and CARD containing protein |
| NLRP | NOD-, LRR- and PYD containing protein |
| oxLDH | oxidised low density lipoprotein |
| P/S | penicillin/streptomycin |
| PA | protective antigen |
| PAMP | pathogen associated molecular pattern |
| PBS | phosphate buffered saline |
| PCR | polymerase chain reaction |
| PD-1 | programmed death protein 1 |
| PD-1L | programmed death protein 1 ligand |
| PMA | phorbol 12-myristate 13-acetate |
| PMSF | phenylmethylsulfonyl fluoride |
| pNA | p-nitroanilide |
| PQQ | pyrroloquinoline quinone |
| Pro | proline |
| PRR | pattern recognition receptor |
| PS | phosphatidylserine |
| PVDF | Polyvinylidene difluoride |
| PYD | pyrin domain |
| RHOA | Ras homolog family member A |
| RNA | ribonucleic acid |
| ROS | reactive oxygen species |
| RPMI | Roswell Park Memorial Institute Medium |
| RT | room temperature |
| SDS | sodium dodecyl sulfate |
| SDS PAGE | sodium dodecyl sulfate polyacrylamide gel electrophoresis |
| SEM | standard error of mean |
| Ser | serine |
| sFAP | soluble fibroblast activating protein |
| T cells | thymus dependent lymphocytes |
| TAA | tumor associated antigen |
| TAN | tumor associated neutrophils |
| TBS | Tris-buffered saline |

| | |
|-------------------|---|
| TBS-T | Tris-buffered saline with Tween20 |
| TGF- β | transforming growth factor β |
| Th | T helper cell |
| TLR | Toll-like receptor |
| TME | tumor microenvironment |
| TNF | tumor necrosis factor |
| Tregs | regulatory T cells |
| VBP | Valboro-Pro |
| VBP | Valboro-pro |
| VEGF | vascular endothelial growth factor |
| WT | wild type |
| YUMM1.7 | Yale University mouse melanoma cell line 1.7 |
| YUMMER1.7 | Yale University mouse melanoma cell line 1.7 exposed to radiation |
| YUMMER1.7- GFP | Yale University mouse melanoma cell line 1.7 exposed to radiation expressing GFP |

Abstract

The world health organization WHO declares cancer as the second leading cause of death globally.^[1-3] Despite the strong research and a vast variety of treatments, 8.8 million people died due to cancer in 2015.^[1] Cancer immunotherapy is the most groundbreaking achievement in cancer treatment of the last two decades.^[4] The striking success with checkpoint inhibitors blocking the cytotoxic T-lymphocyte associate protein 4 (CTLA-4) and the programmed cell death protein 1 (PD1) provoked a boost in the development of new components for cancer immunotherapy.^[4-7] Antibodies against CTLA-4 or PD1 promote T-cell response against cancer, by blocking inhibitory signal transduction of T-lymphocytes.^[4-6, 8] These strategies target the adaptive immune system. In our studies, we showed that the stimulation of the NLR family pyrin domain containing 1 (Nlrp1) inflammasome, an innate immune sensor, is sufficient to mediate tumor regression in mice. We investigated the immunomodulatory drug Valboro-pro, that was previously shown to attenuate tumor growth through a yet unexplored mechanism.^[9] Valboro-pro induces pyroptosis, a lytic form of cell death in murine myeloid cells by inhibiting the serine proteases DPP8 and DPP9.^[10] In this study we demonstrate that the pyroptotic effects of Valboro-pro depend on NLR family pyrin domain containing 1 (Nlrp1) in murine monocytes. We further successfully generated human monocyte knockout cell lines of DPP9, apoptosis associated speck-like protein containing a CARD (ASC), and caspase-1 utilizing CRISPR/Cas9 technology.

This work provides first evidence that the pyroptotic properties of Valboro-pro rely on the activation of Nlrp1. Furthermore, these studies emphasize the potential of targeting inflammasomes as adjuvants to enhance and complement the effects of current cancer immunotherapies.

Keywords: Cancer, Immunotherapy, Inflammasomes, Nlrp1, Serine Proteases, Valboro-pro

Introduction

The immune system evolved to defend the host against invading pathogens.^[11] Apart from foreign organisms, the immune system is further able to detect and eliminate aberrant components of the own body, such as cancer cells, to maintain a healthy organism.^[12] Cancer causes one of six deaths in humans, hence the second leading cause of death globally.^[1-3] The annual total economic costs of cancer was estimated at approximately US\$ 1.16 trillion in 2010.^[1, 13] Available treatments reach from surgery to chemotherapy, radiation and immunotherapy, and are developed constantly.^[4, 14] Cancer-immunotherapy relies on stimulating and (re-)activating the hosts own immune system to enhance tumor clearance and was stated multiple times as the breakthrough of modern oncology.^[4, 5, 14-17] Although successive research has been done in the field of cancer-immunotherapy, we still did not reach the limit of maximum possibilities to enhance immune-driven regression and eradication of tumors through immune-therapeutics.^[4] However, the success of currently applied immune treatments raises high expectations of the future of cancer treatments.

The immunity of cancer

Cancer derives from any abnormally proliferating cells of the body, able to escape the detection and clearance by the immune system of the body.^[12] Tumors can therefore be seen as “self”- derived pathogens and are combated by the same arms of the immune system as foreign invaders.^[12, 18-20] One of the major concepts of immunity, is to be able to discriminate self- from non-self.^[21] Deriving from host cells, malignant cells have inherited advantage of evading recognition by immune system.^[12, 18-21] Immunosurveillance, a concept first described in the early 20th century postulates the major role of the immune system in tumor recognition and clearance.^[22] The theory of immunosurveillance supposes that newly arising tumors are recognized by the immune system through the expression of tumor specific neo-antigens, hence subsequently eliminated.^[22]

Considering the fact that cancer occurs despite a functional immune system, the model of tumor editing provides a more detailed explanation of carcinogenesis, separated in three distinct phases: elimination, equilibrium and escape.^[11, 23] The elimination phase describes the initial idea of immunosurveillance whereby the arising tumor cells are recognized and cleared. This either happens through the recognition of tumor specific

neo-antigens or/and as a result of failed intrinsic tumor suppressor mechanisms. If the elimination of those tumor cells remains incomplete, a state of equilibrium is described, in which the immune system keeps the proliferating cells in check, as such no net outgrowth of malignant cells occurs. In this phase, cancer cells persist and are hypothesized to accumulate further mutations under constant selective pressure of the immune system, mostly mediated by thymus dependent lymphocytes (T cells). If the immune system continues to fail to clear remaining tumor cells, changes within malignant cells, e.g. the loss of major histocompatibility complex (MHC) class I protein, and changes of the tumor environment allow the tumor to escape the surveillance of the immune system.^[11, 12, 23, 24]

Anti-tumor response

Particularly in early stages of cancer development, innate immune cells that recognize cell-surface patterns like natural killer (NK) cells or macrophages are crucial for effective clearance of malignant cells.^[25] Lack of MHC-expression on the surface of newly arising cancer cells leads to the elimination by NK cells through the release of cytotoxic proteins like perforin and granzyme. Apoptotic tumor cells express “eat me” signals, including lipid phosphatidylserine (PS) on the outer layer of the cytoplasmic membrane or oxidized low-density lipoprotein (oxLDH). Those signals are recognized by macrophages and lead to the phagocytosis and elimination of cancer cells.^[25] Dendritic cells (DC), antigen presenting cells and the bridge between the innate and adaptive immune system, recognize and phagocytose “eat me” signal presenting cancer cells, similarly to macrophages.^[25] In their role as connection of the innate and adaptive immune response, DC provoke tumor elimination through presenting tumor associated antigens (TAAs) to T cells or activating cytotoxic T cells effectively by secreting interleukin (IL) 12, IL-23 or IL-1.^[24] Neutrophils, like dendritic cells either kill tumor cells directly or activate the adaptive immune response.^[26] In contrast to dendritic cells, neutrophils kill their targets through the release of nitric oxide production. Activation of cytotoxic T cells occurs through the release of pro-inflammatory factors, such as IL-8, tumor necrosis factor (TNF) α and IL-6.^[26] T cells, together with bursa-dependent lymphocytes (B cells)^[24] part of the adaptive immune system, play a crucial role in tumor clearance. CD4⁺ T helper subsets together with CD8⁺ T lymphocytes mediate direct tumor killing and secretion of anti-tumor associated cytokines interferon (IFN) γ , TNF- α , and IL17.^[24] Tumor associated

antigens are directly recognized by cytotoxic T cells (CTLs) and are displayed on the surface of cancer cells in complex with the human leucocyte antigen (HLA) class 1 molecules.^[27] T helper cells further support the anti-tumor response through the expression and release of IL-2. The administration of IL-2 was celebrated as first effective cancer immunotherapy approach in humans, resulting in increased T cell numbers upon direct administration or adopted transfer of in vitro IL-2 stimulated homogenous T cells.^[28]

Pro-tumorigenic environment

The tumor environment consists not only of cancer cells, but multiple subsets of immune cells, stromal cells together with non-cellular components, collectively referred to as the tumor microenvironment (TME).^[24] Composition and effector function of the TME can be used as curing rate prognosis or provide important information for choosing effective therapeutic approaches.^[24] Cancer associated fibroblasts (CAFs) or myofibroblasts, also involved in wound healing, are constantly activated in the cancer environment.^[24] CAFs promote tumor growth by either directly acting on cancer cells through cytokine and growth factor secretion or by remodeling the extracellular matrix (ECM), induction of angiogenesis or recruitment of immune cells.^[24] Through the release of reactive oxygen or nitrogen species, neutrophils not only kill newly arising tumor cells but also promote tumorigenesis through DNA damage.^[26] The release of the metalloproteinase MMP9 by tumor associated neutrophils (TANs) activates vascular endothelial growth factor (VEGF) and fibroblast growth factor 2 (FGF2) in the TME, hence promoting angiogenesis, supporting the outgrowth of solid tumors.^[26, 29] While macrophages prevent the outgrowth of malignant cells through phagocytosis, several studies have revealed that the depletion M2-type macrophages during tumor induction actually restrained tumor growth.^[30] The M2 or alternatively activated macrophage type is the predominant macrophage in the TME and display a reportedly anti-inflammatory and pro-tumorigenic phenotype.^[30] Dendritic cells can dampen anti-tumor responses by providing anti-inflammatory IL-10 and TGF- β .^[27, 31] TGF- β is the promoter of regulatory T cells (Tregs). Regulatory T cells are Foxp3 marked immunosuppressive lymphocytes crucial in preventing autoimmunity and excessive inflammation. Hence, vast tumor infiltration by Tregs is associated with poor survival prognosis in patients.^[31]

Repeated stimulation of T cells driven by cancer development and chronic infection can lead to a dysfunctional state termed T cell exhaustion, eventuating in impaired tumor recognition and clearance.^[32] Therefore, important mechanisms by which malignant cells are capable of evading the immune system are the upregulation of inhibitory receptor proteins like programmed death-1 (PD-1) that promote T cell exhaustion.^[6, 32] These receptor-ligand interactions function as “checkpoints”, coordinating whether or not T cells should differentiate and exert their effector functions.^[6, 8] Consequently, upregulation of PD-1 ligand (PD-1L) on cancer and antigen presenting cells (APCs) dampens an anti-tumorigenic effect.^[5, 6]

Immunotherapy as cancer treatment

The first therapeutic that adjuvants the immune system to recognize and eliminate tumors was a mixture of heat-killed bacterial strains developed by William B. Coley, MD in 1893.^[27, 33] William B. Coley developed the “Coley’s toxins” after his observation that the tumor of one of his patients regressed after the patient underwent a bacterial infection with *Streptococcus*.^[27] Although B and T cells were not known around this time, it is standing to reason that the strong infection caused by streptococcus infections boosted the immune system of the patient and this led to subsequent clearance of the tumor.

Over the last decades, developing novel therapies to activate the immune system to fight cancer was a strong focus of cancer immunology and oncology.^[27] The administration of immune-stimulating cytokines like IL-2 and IFN- α was the first step towards modern cancer immunotherapy.^[28] In addition to providing cytokines that modulate the immune system, another strikingly successful approach is to block checkpoints that would otherwise result in a reduced anti-tumor T cell response. The natural science journal *Science* stated checkpoint inhibitor blockade as the “Breakthrough of the Year” in 2013.^[27, 33] Antibodies like Ipilimumab and Nivolumab target the immune checkpoint inhibitor cytotoxic T-lymphocyte-associated antigen 4 (CTLA4) and PDL-1, respectively. The immune checkpoint inhibitor CTLA4 was the first one clinically targeted in cancer immunotherapy and is exclusively expressed on T cells.^[5] Highly expressed on CD8+ T cells as well as CD4+ T helper (Th) subsets and Tregs, this receptor counteracts the activity of the T cell co-stimulatory receptor, CD28.^[5] Checkpoint inhibitor blockades targeting CTLA4 (Ipilimumab) and PDL-1 (Nivolumab) are therefore considered to be the major improvement in modern cancer

immunotherapy, displaying potent anti-tumor effects in multiple cancer. The concept of immunotherapy is to reactivate the patient's own anti-tumorigenic response. Besides checkpoint inhibitor blockades that counteract suppressive stimuli that reduce effective recognition and clearance, enhancing T cell numbers and infiltration potential of lymphocytes are crucial steps in successful treatment approaches. In addition, high numbers of tumor infiltrating lymphocytes are associated with positive outcomes of treatment.^[24] Combination therapies of Ipilimumab, Nivolumab, IL-2, radiation or common chemotherapy are widely used to provide the best chances for effective tumor clearance.^[34]

The dual role of inflammation in tumor progression and surveillance

Inflammation is a host derived immune response evoked by bacterial, viral and fungal infections or sterile stimuli.^[35] Pathogen or danger associated molecular patterns (PAMPS, DAMPS) are recognized via specific pattern recognition receptors (PRRs), including Toll-like receptors (TLRs), NOD-like receptors (NLRs) and the receptor family absent in melanoma 2 (AIM2). In addition, emerging data advances our understanding of sensing homeostatic perturbations for there are no determined PRRs (homeostasis-altering molecular pathways; HAMPs), withal considered as sterile stimuli for inflammation. Activation of cells through these pathways subsequently results in the release of cytokines and the recruitment of multiple immune cell subsets culminating in an inflammatory response. Inflammation displays a dual role in cancer development and immunosurveillance. Acute, restrained inflammation, mediated by cytokines like IL-4 or IFN- α , NKs and DCs has been reported to promote tumor clearance.^[15, 18] On the other hand, chronic sustained inflammation, associated with unrestrained innate immune response or dysregulated adaptive response can generate a pro-tumorigenic environment.^[11, 15, 18] Chronic inflammation in the gut reportedly leads to increased tumor incidences, and cancer itself is described as chronic disease presenting with inflammation.^[26, 36] Nevertheless, immunotherapy purposefully induces inflammation to boost an inflammatory immune response aiming to clear tumors.

Immune checkpoint inhibitor blockades and treatments with T-cell stimulating cytokines target the adaptive immune response. However, cells of the innate immune system are naturally the first responders to pathogen invasion and likewise the first inducers of inflammation.^[37] Elucidating the mechanistic action and role of the innate immune system in the prospect of cancer development, novel findings might provide

important information how to modulate the immune response to emerging tumors or fine-tune and improve current immunotherapies against established cancers.

Inflammasomes: Intracellular sensor platforms driving inflammation

Inflammasomes are multiprotein complexes that assemble after ligand binding/sensing and lead to the activation of inflammation driving caspases, resulting in the maturation and cleavage of pro-inflammatory cytokines.^[38, 39] A diverse set of intracellular proteins recognizing PAMPs, DMAPs or HAMPs feed into the single response pathway “inflammasome”.^[40, 41] These PRRs include AIM2, NLRC4 (NOD-, LRR- and caspase activation and recruitment domain-containing) protein 4, NLRP1 (NOD-, LRR- and pyrin domain-containing) protein 1, NLRP3, NLRP6 and pyrin. All these inflammasome sensors share the same concept of signal transduction. Upon ligand binding, these sensors oligomerize and lead to the recruitment and subsequent activation of the pro-inflammatory protease caspase-1.^[42, 43] In order to mediate interaction with the effector molecule caspase-1, all sensors recruit the apoptosis-associated speck-like protein containing a CARD (ASC). ASC contains two death fold domains, one pyrin domain (PYD) and a caspase activation and recruitment domain (CARD). With these two domains, ASC bridges the upstream activated inflammasome sensors and caspase-1 (Schematics, Figure 1).



Figure 1 Simplified schematics of possible inflammasome complex containing ASC and caspase-1. Scheme was created by the author of this thesis and designed inspired by Broz and Dixit^[38]

Recruitment of the adaptor molecule ASC correlates with the oligomerization of ASC through homotypic PYD-PYD and CARD-CARD interactions. This aggregation into a single macromolecule is known as ASC speck and is formed regardless of the identity of the upstream activated inflammasome sensor.^[38, 39] Pro-caspase-1 is recruited to the complex via the CARD domain and is activated through proximity induced autoproteolytic cleavage. Upon activation, caspase-1 processes its substrates pro-IL-1 β and pro-IL-18 into their mature form. IL-1 β , is a potent proinflammatory cytokine and known inducer of Neutrophil infiltration.^[26, 44] IL-18 has been shown to have both,

inflammatory and regulatory functions.^[45, 46] In macrophages, IL-18 induces the production and release of additional pro-inflammatory cytokines. IL-18 in conjunction with IL-12 or IL-15 induces IFN- γ production by CD4⁺ T cells. Alternatively, in the absence of those cytokines, IL-18 triggers the production of anti-inflammatory cytokines such as IL-13 and IL-4.^[45]

An additional important substrate of caspase-1 is the pyroptotic factor gasdermin D (GSDMD). Cleavage by caspase 1 generates N- and C- terminal fragments of GSDMD. The N-terminal fragments accumulate and then oligomerize to form a pore in the plasma membrane of the cell, inducing lytic cell death.^[45] Multiple studies demonstrated that GSDMD is essential for caspase-1 induced pyroptosis.^[47] Pyroptosis is a lytic form of cell death that is characterized by cell swelling, lysis and the release of cytoplasmic content, hence driving inflammation.^[48-50]

Therefore, activation of inflammasomes and downstream activation of caspase-1, leads to inflammation through the production and release of pro-inflammatory cytokines and an inflammation inducing lytic cell death program.^[48]

The NLRP1 inflammasome and its role in autoinflammation

Inflammasomes respond to various PAMPs and DAMPs, including flagellin (PAMP, NLRC4), microbial and autogenous cytosolic double stranded DNA (PAMP, AIM2), alterations in actin polymerization due to RHOA inactivation by bacterial toxins or infecter proteins (DAMP, pyrin) or potassium efflux (DAMP, NLRP3).^[38] The NLRP1 inflammasome was the first NOD-like receptor to be shown to form an inflammasome complex.^[42] The human NLRP1 consists of a N-terminal pyrin domain (PYD) followed by a 240 amino acid sequence that links the death superfamily domain member PYD to the prototypic NLR NACHT domain and adjacent leucine rich repeats (LRRs).^[51-53] The NLRP1 inflammasome sensor possesses seven LLRs that are followed by a function to find (FIIND) domain that is unique to NLRP1 and CARD8 in humans.^[54] Together with the inflammasome sensor NLRC4, NLRP1 is the only NLR containing a caspase activation and recruitment domain (CARD). The CARD domain of NLRP1 is located on the C- terminus and is either able to recruit the apoptosis-associated speck-like protein containing a CARD (ASC) to mediate caspase-1 (CASP1) activation or to directly activate CASP1.^[55] Of note, the well-studied NLRP3 inflammasome, together with NLRP6, AIM2 and pyrin do not possess a CARD domain and are therefore unable to directly activate caspase-1.^[38]

Although the NLRP1 inflammasome was the first sensor to be discovered, the activators remain to be elucidated. In mice, the homologous sensor Nlrp1b has been shown to be activated by the lethal factor (LF) of *Bacillus anthracis* and *Toxoplasma gondii* infection.^[56, 57] This susceptibility differs between the 5 known generic variants of Nlrp1b in different mouse strains. Furthermore, three paralogues, Nlrp1a, Nlrp1b and Nlrp1c are described in mice, in contrast to human that only possess one NLRP1 gene. Although they share the general domain structure of NACHT, LRRs, FIIND and CARD, the human N-terminal PYD is replaced by a NR100 domain and a notably shortened linker region connects this NR100 to the NACHT domain. Although the mouse paralogue Nlrp1a and the human NLRP1 are not activated by LF, studies in the mechanistic action of *B. anthracis* induced pyroptosis revealed that cleavage of the N-terminus of Nlrp1b is required for inflammasome activation. Engineering this cleavage site into Nlrp1a and NLRP1, showed that cleavage of the N-terminus also leads to activation in these variants, uncovering an autoinhibitory function of the N-terminus.^[52] In addition, studies in human and mice presented evidence that disrupting mutations of the PYD or NR100 linker domain in Nlrp1a, lead to auto-inflammation, driving diseases like multiple self-healing palmoplantar carcinoma (MSPC), familial keratosis lichenoides chronica (FKLC) or cytopenia.^[46, 51, 58] Patients displaying MSPC or FKLC were shown to carry dominant mutations in the PYD domain and that this domain, if intact, displays autoinhibitory functions and prevents inflammasome oligomerization. Therefore, mutations in this domain lead to abrogated autoinhibition and exaggerated inflammasome activation. In addition to chronic skin inflammation conditions and warty keratoacanthomas, keratinocyte cultures of these patients showed increase ASC speck formation and the release of the pro-inflammatory cytokines IL-1 α , IL-1 β and IL-18. These studies provided first evidence to link NLRP1 hyperactivation to inflammatory skin disorders and skin cancer predisposition.^[46] In addition to the skin, Nlrp1a is further highly expressed in the hematopoietic cell compartment. An N-ethyl-N-nitrosourea (ENU) mutagenesis screen for dominant mutations revealed that a single amino acid substitution in the linker domain between NACHT and LRR in Nlrp1a causes neutrophilia in mice by leading to a constitutively active inflammasome. These mice displayed a shorter live span compared to wild-type (WT) mice, dependent on IL-1 β . In addition, Nlrp1a mutants increase IL-18 serum levels, but knocking out IL-18 worsens their disease, indicating a negative regulatory function of IL-18. Interestingly,

however, this study suggests cell-intrinsic roles for NLRP1a-induced pyroptosis in hematopoietic progenitor cells independently of ASC or caspase 11.^[46]

Inflammasomes as targets in cancer-immunotherapy

Functioning as innate immune sensors that induce inflammation, inflammasomes are promising targets for immunotherapy. Multiple studies correlated inflammasome signaling with altered prognosis in tumor models. The loss of Nlrp3 in an azoxymethane-dextran sulfate sodium (AOM-DSS) induced colitis model increased the tumor incidence of colorectal carcinomas and further enhanced the outgrowth of metastatic foci in the liver because of impaired IL-18 signaling.^[20] Knockout of Nlrp4 and the effector protein Casp1 in the same model, proposed reduced inflammation-induced tumorigenesis after injury due to intrinsic effects in the colorectal epithelium.^[36] Astonishing findings of the Canakinumab Anti-inflammatory Thrombosis Outcomes Study (CANTOS), published in the general medicine journal Lancet 2017, revealed that treatment with the IL-1 β antibody canakinumab over the course of 3.7 years reduced the incidence of lung cancer by 67%.^[59, 60] This study, originally designed to elucidate the effect of IL-1 β inhibition in atherosclerosis further uncovered the promoting role of IL-1 β - a major product of inflammasome activation- in tumor growth, invasiveness of malignant cells and metastatic spread. Taken together, these findings point out the vast potential of inflammasome targeting in optimizing cancer immunotherapy and augmenting the understanding of innate induced inflammation in tumor progression.

Dipeptidyl Peptidases, a diverse protease family involved in inflammation, metabolism and homeostasis

Dipeptidyl Peptidases (DPPs) are N-terminal exopeptidases, that cleave off a dipeptide of the N-terminus of their substrates.^[61] The prototypic DPP, DPP4, and its family members have been extensively studied over the past 50 years and revealed important contribution in pathophysiological and immunological processes.^[62] DPP4 was first isolated from rat kidney and became a propitious target in diabetes type 2 treatment due to its capability to cleave the incretin glucagon- like peptide 1 (GLP-1), a major regulator of glucose homeostasis *in vivo*.^[63, 64] Therefore, inhibitors of DPP4 like sitagliptin, saxagliptin or saxagliptin have become important therapeutic agents against

type 2 diabetes, by regulating blood glucose levels and gluconeogenesis.^[65, 66] Research on DPP4 and other peptidyl peptidases of this family exposed their broad contribution in tumorigenesis, metabolism and inflammatory diseases, thereby exaggerating the broad interest in further studying these proteins as important modulators in disease and health.^[62, 67-70]

DPP4 family members: DPP8, DPP9 and FAP

Members of the DPP4 family are serine proteases with a preference for proline (Pro) or alanine (Ala) at the penultimate position of the N- terminus. In strict terms, the peptidyl peptidases DPP4, DPP4 like protein-1 and 2 (DPP6 and DPP10, respectively), fibroblast activating protein alpha (FAP), DPP8 and DPP9 are the only family members.^[62, 68] These peptidases belong to the serine protease clan SC subfamily 9b, holding a catalytic triad ordered serine (Ser) aspartic acid (Asp) and histidine (His). In broader terms, considering sequence similarity and substrate specificity, the prolyl oligopeptidase PREP, and the prolyl carboxypeptidase PRCP can be further classified as DPP4 family members.^[62]

FAP exists like DPP4 as transmembrane protein or secreted soluble form (sFAP). In addition to its exopeptidase activity, FAP also displays gelatinase function which allows for degradation of the ECM. Highly expressed in the tumor associated fibroblasts of most solid tumors and in 90 % of human epithelial cancers, FAP is involved in tissue remodeling and has shown to support tumor growth and metastasis.^[67, 71]

The family members DPP8 and DPP9 are cytosolic with few reports of DPP9 being detected also in the nucleus. DPP8 and 9 display 77% sequence similarity and despite their close relation and overlapping substrate specificity with DPP4, they are potentially involved in distinct physiological pathways due to their separate localization. Several studies aimed to unravel potential targets and substrates of these serine proteases to elucidate their function.^[62, 72, 73] While these studies provided excessive lists of possible substrates, pathways inheriting cleavage by DPP8 or 9 as crucial factors for signal transduction, remain to be elucidated. DPP8 and 9 work as dimers and are sensitive to changes of redox potential.^[74, 75] Oxidation of sulfhydryl groups of cysteines surrounding the catalytic center of these serine proteases leads to strong inhibition of DPP8/9 activity but not in DPP4. Redox-responsiveness in these studies was assayed in vitro through the addition of reactive oxygen species (ROS) like H₂O₂ or the bacterial coenzyme pyrroloquinoline quinone (PQQ). PQQ is a coenzyme of several bacterial

dehydrogenases and oxidizes neighboring cysteinyl residues to disulfide bonds.^[75] These experiments showed a potential role of DPP8/9 in sensing the redox status of the cell. Stress conditions resulting in mitochondrial or endoplasmic reticulum mediated stress can increase cytosolic ROS. These perturbations in ROS abundance could be a result of infection or metabolic stress. In addition, sterile stimuli like UV-radiation can further enhance ROS levels.

DPP9 is considered to be the rate limiting endopeptidase in the degradation of proline-containing peptides.^[76] Moreover, mice homozygous for a catalytic inactive mutation of DPP9 die within 8-24 hours after birth, probably attributable to metabolic impairment.^[77] Others report that the knock-in of the same catalytic mutant lead to a defect in tongue development. Lack of catalytically active DPP9 results in increased cell death of migratory muscle progenitor cells. As a consequence, mice expressing this DPP9 mutant succumb to neonatal lethality due to a suckling defect.^[78]

Although the DPP4 family member display a very specific substrate specificity, FAP, DPP4/8/9 contribute to various distinct processes within cells and organisms, pointing out the great potential for further investigation in the context of metabolic diseases, cancer development and stress responses.

Inhibitors of Dipeptidyl Peptidases

Inhibitors of dipeptidyl peptidases already expose a wide range of applications as metabolic and immunological modulators. DPP4 inhibitors are approved and widely approached as diabetes type 2 treatments. Moreover, inhibition of DPP4 has recently been shown to enhance lymphocyte trafficking by increasing levels of biologically active CXCL10.^[79] CXCL10, a chemokine, mediates lymphocyte trafficking into tumor tissue through signaling of its receptor CXCR3, enhancing an anti-tumor response in melanoma models. N-terminal truncation of CXCL10 through Dpp4 leads to a dominant negative form of this cytokine which negatively affects T cell trafficking to tumor sites.^[79] Treatment with anti-FAP antibodies revealed positive effects in melanoma, breast and pancreatic cancer, all together demonstrating the potential for DPP family members as target for future immunotherapies.^[65, 67, 71, 79]

Valboro-Pro

Valboro-Pro (VBP, Figure 2), also referred to as Talabostat or PT-100, is a nonspecific serine protease inhibitor that has generated considerable interest based on its ability to enhance T cell mediated tumor clearance.^[80] The amino-boronic dipeptide competitively inhibits the dipeptidyl peptidase activity of a wide variety of serine proteases, including DPP4, DPP7, DPP8, DPP9, FAP, PREP, SCPEP1, through high affinity binding to the active site, mediated by complex formation between the serine of the catalytic triade of its target with the intrinsic boronic acid.^[81]

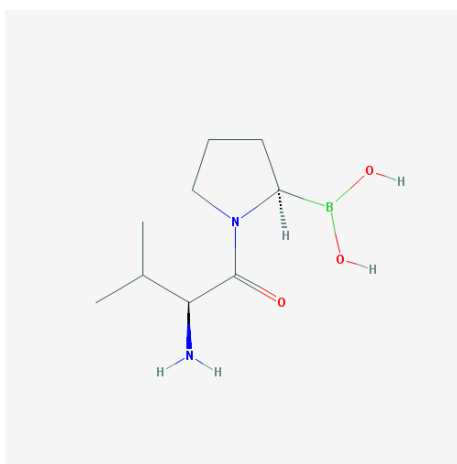


Figure 2 Structure of Valboro-pro. Source: PubChem; URL: <https://pubchem.ncbi.nlm.nih.gov>

Multiple lines of evidence indicate that VBP kills cancer cells indirectly by enhancing an anti-tumor immune response.^[80, 82] VBP administration reduces tumor growth of multiple syngeneic models in vivo but does not influence tumor cell growth in vitro. In addition to growth restriction, administration of VBP leads to complete tumor clearance in several conducted syngeneic tumor experiments.^[80, 82] Moreover, female C57BL/6 mice further acquire an adaptive immune response against MB49, protecting mice of further tumor growth upon re-challenge after 56 days after initial tumor induction.^[80] The in vivo effect of the chemical component depends on dendritic cells and T cells and is believed to occur by enhancing early dendritic cell migration to tumor infiltrating lymph nodes and an acceleration of T cell priming.^[80, 82]

In addition with other cytokine levels, Adams et al. assayed the effect of DPP4 (also named CD26) on tumor regression. Although they report no major contribution of DPP4 in the observed phenotype and claim an CD26 independent mechanism of VBP tumor growth restriction, their reported data leave room for alternative interpretation. Herein, other studies revealed that DPP4 knockout in mice enhances reduction of tumor

incidences^[79], indicating that VBP might function by inhibiting other DPP family members or DPP inhibition can exacerbate its effect. Exploiting the high-throughput, superfamily-wide multiplexed profiling method EnPlex, DPP4, 8 and 9 have been defined as strongest targets for VBP mediated inhibition.^[10] This study demonstrated that VBP induces pyroptosis, a lytic form of cell death, in a panel of immortalized myeloid cell lines, proposing new possibilities to explain the anti-tumor effects of VBP that remain to be determined.^[10]

Serine Proteases as Inflammasome modulators

Recent studies of Okondo et al., demonstrated that VBP induces pyroptosis in hematopoietic cells.^[10] The pyroptotic effects of VBP are dependent on caspase-1, but not caspase 4 and 5, mediators of a non-canonical pyroptotic pathway which responds to lipopolysaccharide (LPS). In addition, DPP8 and 9 were identified as the VBP inhibition target responsible for activating caspase-1. In the proposed model, DPP8/9 inhibition by VBP leads to the activation of pro-caspase-1 through an unknown mechanism. Knockout of DPP9 and DPP8/9 double knockout, but not DPP4, leads to increased LDH release in THP1 cells without further stimulation with VBP.^[10]

To determine if DPP8 and 9 and if other DPP members are expressed in mouse derived primary macrophages, the Flavell Lab performed RNA-sequencing on mouse bone marrow derived macrophages of C57BL/6 mice. RNA-sequencing results preliminarily generated by the Flavell-Lab revealed expression of DPP8 and DPP9 in primary mouse derived macrophages (Figure 3).

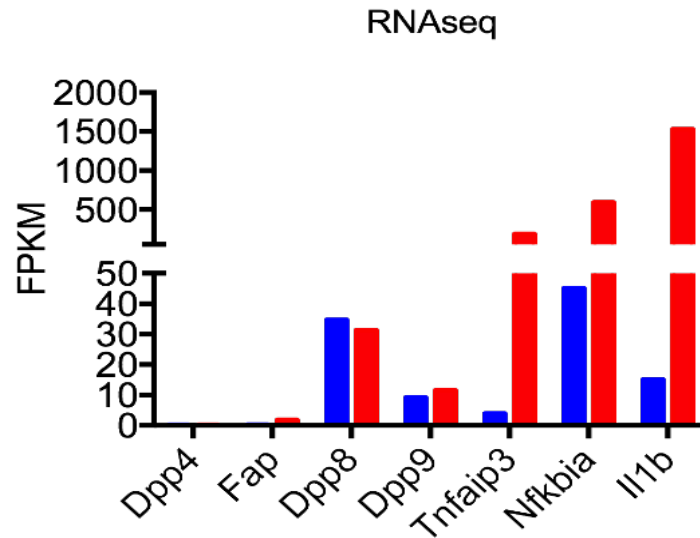


Figure 3 Mouse derived primary macrophages express DPP8 and DPP9. RNA Sequencing of mBMDMs; unpublished data generated and provided by the Flavell Lab.

Caspase-1 is an effector molecule downstream of inflammasome signaling. Screening for responsiveness to VBP in several mouse and human derived myeloid cell lines by Okondo et al. displayed high responsiveness of RAW264.7 cells to VBP.^[10] RAW264.7 cells do not express ASC, the adaptor protein mediating the assembly of an inflammasome-caspase complex.^[83] Knockout of ASC in mBMDMs revealed the partial independence of ASC in VBP induced pyroptosis in mBMDMs (Okondo et al. 2017 and Figure 5). Only the inflammasome sensors Nlrp1 and Nlrc4 can directly interact with caspase 1 through their internal CARD domain, leading to the hypothesis of contribution of one or both to VBP induced cell death. Further experimental data generated by the Post Doc. James Richard Brewer demonstrated that Nlrc4 does not mediate cell death upon VBP treatment in mBMDMs (Figure 4).

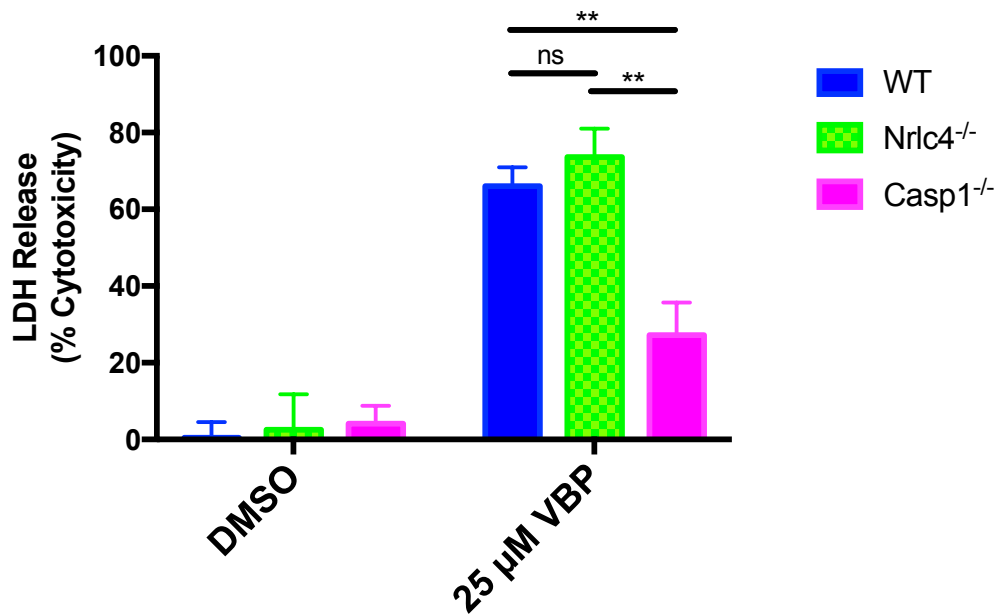


Figure 4 VBP leads to LDH release in WT and Nlr4^{-/-}, but not Casp1^{-/-} mBMDMs. mBMDMs were treated with 25μM VBP for 24 hours. Statistical significance was assayed with Student's t-test. **p<0.005

Activation of caspase-1 and induction of pyroptosis are characteristics of inflammasome activation. Therefore, it remains to be elucidated if VBP induces pyroptosis in dependence of the activation of an inflammasome sensor. It is of interest to determine which inflammasome sensor can mediate pyroptosis upon DPP8/9 inhibition caused by VBP treatment. Investigating the mechanistic way of action of VBP may give further insights into the biological activity in cancer models. Knowledge gained could be important for unraveling the contribution of innate immune signaling to tumor clearance upon VBP.

Materials and Methods

Mouse Models

All mice used were on the C57BL/6 background. Nlrp1^{-/-} mice were generated on a 129 background by targeting exon 1-3 to disrupt gene function.^[84] 129 mice encode non-functional Nlrp1a and Nlrp1c gene variants; therefore, inactivation of the functional Nlrp1 gene results in a complete Nlrp1 knockout. Nlrp1^{-/-} mice were backcrossed to C57BL/6J, maintaining complete Nlrp1 loss in this colony on a C57BL/6J background.^[84] Casp1^{-/-} mice were generated by Case et al. 2011, by flanking exon 6 and 7 that encode the catalytic center with loxP sites.^[85] Floxed mice were crossed to C57BL/6N mice encoding Cre under the promoter E2A, purchased from Jax, leading to the deletion of the floxed region.^[85] ASC^{-/-} mice were generated as described in Sutterwala et al. 2006^[86] and backcrossed to C57BL/6N. All mice were bred and maintained under specific pathogen-free conditions at the animal facility of Yale University School of Medicine.

Cell Lines

THP1 cells were purchased from ATCC and handled according to provider's instructions. In brief, THP1 cells were cultivated Eppendorf tissue culture flasks, in RPMI supplemented with 10% fetal bovine serum (FBS), 100 µg/mL penicillin/streptomycin (P/S) plus L-Glutamine (full RPMI media). For differentiation into monocytes and macrophages, THP1 cells were cultured 3 days in full RPMI media with 80 nm phorbol- 12-myristate- 13-acetate (PMA, Sigma P1585). HEK293FS* cells were kindly provided by the Joshi Laboratory of the Yale University School of Medicine. Irradiated Yale university mouse melanoma cells 1.7 (YUMMER1.7) and YUMMER1.7 cells expressing GFP (YUMMER1.7-GFP) were provided by the Bosenberg Laboratory^[87] (Dermatology Department, Yale School of Medicine). MC38 cells were kindly provided by the Bosenberg Laboratory and EL4 cells were purchased from ATCC, both cultivated in DMEM supplemented with 10% FBS and 100 µg/ml P/S.

Reagents

Valbora-Pro (VBP; Talabostat mesylate) was purchased from MedKoo Biosciences. For tissue culture, VBP was reconstituted in DMSO and stored at -20°C. For the tumor

experiments, 200µg Valboro-Pro (VBP) were dissolved in 0.1N HCl and diluted to a final concentration of 20µg/150µl with 0.9% NaCl. Single dose administration for cytokine detection in serum was performed with 100µg VBP in 150µl vehicle p.o.

The chromogenic substrate Gly-Pro p-nitroanilide was purchased from Sigma-Aldrich (# G0513) and used as indicated. LPS (Enzo, ALX-581-012-L002) and nigericine (Invivogen, tlr1-nig) were used as indicated.

Tumor Models

6-9 weeks old mice were shaved at injection side prior to injection. 5×10^5 cells (EL4, MC38, YUMMER1.7-GFP, YUMMER1.7) suspended in 100 µl Dulbecco's PBS (DPBS) were injected subcutaneously. Mice of different genotypes and treatments were cohoused as indicated to control for effects caused by diverging microbiota. 20µg VBP, were administered p.o. twice daily at an interval of approximately 8 hours. Tumor sizes were determined by measuring the greatest length of tumors (length) and the perpendicular longitude (width) with a caliper. Tumor volume was estimated according to the formula: $width^2 \times \frac{length}{2}$. Mice were euthanized at a humane endpoint of 2cm tumor length in any direction or when tumors became ulcerated.

Generation of Mouse Bone Marrow Derived Macrophages

Bone marrow was collected of mice at an age of 5-12 weeks. Mice were sacrificed and femur and tibia isolated by removing skin and muscle. The bones were kept in ice cold phosphate buffered saline (PBS) till further processing. To isolate bone marrow, the tips of the bones were cut and flushed with DMEM substituted with 10% FBS, 100 µg/ml P/S, 2mM L-glutamine and 50ng/ml macrophage colony stimulating factor (M-CSF, BioLegend 576404). At day 4-5 after isolation, fresh MCSF full DMEM media was added to sustain growth factor required for macrophage differentiation. BMDMs were utilized between day 8-12 after isolation for experiments.

Cytokine detection with ELISA

To assay serum cytokine levels, blood of mice was collected via terminal cardiac puncture. Samples were incubated on ice for one hour and centrifuged at 21000 g at 4°C for 10 minutes. Serum was transferred into new tubes and stored at -80°C for further use. Supernatants collected from tissue culture were collected and filtered

(0.2µm) prior to cytokine assessment. To assay cytokine levels at tumor sites, we isolated tumors post mortem and reduced them to small pieces of 1mm³. Minced tumor was then incubated in PBS (volume dependent on tumor weight, 1mg tumor corresponds to 2µl PBS) at 37°C for 1h. Suspension was centrifuged 21000 g at RT and interstitial fluid was harvested and stored at -80°C until further use.

Elisa kits for cytokine level evaluation were purchased from different manufactures as indicated in Table 1 and performed accordingly to the manufacturer's protocol.

Table 1 ELISA kits for cytokine detection

| Reagent or Resource | Source | Identifier |
|---------------------|---------------|-------------|
| Mouse IL-1β | R&D SYSTEMS | DY401-05 |
| Mouse IL-18 | Thermo Fisher | BMS618-3TEN |
| Mouse CXCL1 | R&D SYSTEMS | DY453 |
| Mouse CXCL10 | R&D SYSTEMS | DY466-05 |
| Mouse IFN-γ | R&D SYSTEMS | DY008 |
| Mouse IL-1Ra | R&D SYSTEMS | DY480 |

Generation of THP1 KO cell lines for DPPs and inflammasome components

CRISPR/Cas-9 technology utilizing lentiviralCRISPRv2 system developed by Zhang et al 2014 (Addgene, plasmid #52961)^[88] was used to knock out serine proteases and inflammasome components of interest in THP1 cells. To control for efficient transduction, a lentiGFP construct (pLenti CMV GFP Puro 658-5), a gift from Eric Campeau & Paul Kaufman (Addgene plasmid # 17448)^[89] was utilized. The serine protease DPP9 and the pyrin-domain adaptor protein ASC was knocked-out using a single guide strategy; knockouts were confirmed via western blot, or a combination of functional readout and sequencing. In the absence of specific antibodies for human caspase-1 and human NLRP1, a two guide Cas-9 strategy was attempted, targeting either the full locus or exons leading to a predicted frameshift and therefore truncated proteins through the introduction of premature stop codons.

Cells were cloned after selection (100 ng/ml puromycin, InvivoGen ant-pr-1; 100 ng/ml neomycin, InvivoGen ant-gn-1) to derive cell populations from single clones. Constructs for CRISPR/Cas9 targeting as well as all primers used in this project are listed below.

lentiCRISPRv2 single guide targeting

The lentiCRISPRv2 one vector system encodes an expression cassette for the humanized *S. pyogenes* Cas9 and a separate cassette for the expression of the guide RNAs.^[88] Plasmid was cut with BsmB1 restriction enzyme and dephosphorylated to reduce probability of religation. Oligonucleotides were designed against targeting sequences flanked by complement sequences of BsmB1 digested plasmid overhangs, 20-mer of target specific guide RNAs are listed in Table 2. CAS-Designer of CRISPR RGEN Tools [Biology Software] (2017/2018, retrieved from <http://www.rgenome.net>) and Benchling [Biology Software] (2017/2018, retrieved from <https://www.benchling.com>) CRISPR design tool was utilized to determine suited guide RNA sequences. Annealed and phosphorylated oligonucleotides were ligated into the purified BsmB1 digested vector and transformed into Stbl3 (Invitrogen, # C737303), recombinant-deficient *E. coli*.

Table 2 guideRNA sequences for 1-guided CRISPR/Cas9 targeting in THP1 cells

| Target | Oligo name | 5'-3' Sequence | Source/ designing tool |
|--------|------------|-----------------------|---------------------------|
| Exon 4 | hNLRP1sg1a | GTCGCATAGTCATACTGCAGG | Rgenome |
| | hNLRP1sg1b | CCTGCAGTATGACTATGCGA | Rgenome |
| Exon 4 | hNLRP1sg2a | GCTCGCATAGTCATACTGCAG | Rgenome |
| | hNLRP1sg2b | CTGCAGTATGACTATGCGAG | Rgenome |
| Exon 2 | hNLRP1sg3b | GCTGGATCCATGAATTGCCGG | Rgenome |
| | hNLRP1sg3a | CCGGCAATTCATGGATCCAG | Rgenome |
| Exon 3 | hASCsg2a | GCCCTCGCGATAAGCGCAGCC | Okondo et al. 2017 |
| | hASCsg2b | GGCTGCGCTTATCGCGAGGG | Okondo et al. 2017 |
| Exon 2 | hCASP1sg1a | GCTAAACAGACAAGGTCCTGA | Okondo et al. 2017 |
| | hCASP1sg1b | TCAGGACCTTGTCTGTTTAG | Okondo et al. 2017 |
| Exon 2 | mCASP1sg1a | GTTAAACAGACAAGATCCTGA | Okondo et al. 2017 |
| | mCASP1sg1b | TCAGGATCTTGTCTGTTTAA | Okondo et al. 2017 |
| Exon 2 | hCASP1sg2a | GAAAGCTGTTTATCCGTTCCA | Okondo et al. 2017 |
| | hCASP1sg2b | TGGAACGGATAAACAGCTTT | Okondo et al. 2017 |
| Exon 6 | hDPP9sg1a | CGGACTCGTATCGGTACCCC | Okondo et al. 2017 |
| | hDPP9sg1b | GGGGTACCGATAACGAGTCCG | Okondo et al. 2017 |
| Exon 4 | hDPP9sg2a | GGCCAACATCGAGACAGGCG | Okondo et al. 2017 |
| | hDPP9sg2b | CGCCTGTCTCGATGTTGGCC | Okondo et al. 2017 |

lentiCRISPRv2 two guide strategy

In order to target a specific locus, two guides were cloned into the lentiCRISPRv2 backbone under individual U6 promoters, separated by polymerase blockers. PCR template was obtained from other constructs generated by the Flavell Lab.

Guide RNAs designed for the two-guide strategy are listed in Table 3.

Table 3 guideRNA sequences for 2-guided CRISPR/Cas9 targeting of human Nlrp1

| Target | Oligo name | 5'-3' Sequence | Source/ designing tool |
|--------------|-------------------|----------------------|---------------------------|
| Full KO | hNLRP1 5'UTR 2 | TACAGATAGACGCCGATAGA | benchling |
| | hNLRP1 3'UTR 1 | TCCACCGGATTGTCGTAGAG | benchling |
| Exon 1 KO | hNLRP1 5'UTR 1 | TGCTGCAGCGTCAGCTGGTC | benchling |
| | hNLRP1 Intron 1-2 | CATCAATACTCGTGCCTGAA | benchling |
| Exon 4 KO | hNLRP1 Intron 3-4 | GGACAACAGAGCAAGGAGAG | benchling |
| | hNLRP1 Intron 4-5 | ACCTGCCAGTAAGATTCCCA | benchling |

Virus generation for CRISPR/Cas9 targeting and transduction in THP1 cells

Virus generation in HEK293 FS cells*

To generate virus for CRISPR/Cas9 targeting of desired genes in THP1 cells, HEK293 FS* cells were cultured in 15 cm tissue culture dishes to 80-90% confluence in DMEM, 10% FBS, 100 µg/mL P/S. These cells were transfected with lentivCRISPRv2 plasmid construct together with pMD2.G (Addgene, #12259) for VSV-G envelope expression and psPAX2 packaging vector encoding HIV-1 gag and HIV-1 pol (Addgene, #12260) using LipoD293TM transfection agent (SignaGen Laboratories, #SL100668) following manufacturer's instructions. In brief, 20 µg DNA (10 µg LentiCRISPRv2 PURO, 2.5 µg pMD2.G VSVG, 7.5 µg psPAX2 GAG Pol) were combined in 1 ml DMEM only (without FBS or P/S). 50 µl LipoD293TM DNA In Vitro Transfection Reagent in 1 ml DMEM only was quickly combined with 1 ml plasmid mix, vortexed and incubated at RT for 10 minutes. Cells were transfected with reagent mixture in 25 ml fresh DMEM, 10% FBS, 100 µg/mL P/S. Virus was harvested 24-72 hours after transfection by collecting media and filtering through 0.22µm sterile filter (Millipore).

Lentiviral transduction in THP1 cells

To control for successful viral transduction a lentivirus construct containing GFP was transfected in HEK293 FS* in parallel to desired guide constructs. 2.25×10^6

undifferentiated THP1 cells were seeded in 2 ml RPMI containing 25 mM 4-(2-hydroxyethyl)-1-piperazineethanesulfonic acid (HEPES) with 10 µg/ml polybrene and combined with equal volume of harvested virus. Cells were transduced by centrifugation at 2500 rpm (Eppendorf, Germany) at 37°C for 90 minutes. Subsequent to transduction, cells were washed twice with PBS and resuspended in 2 ml RPMI-HEPES and incubated 48 before selection. Transfection efficiency was assayed by determining GFP expression in control assay. To establish THP1 cell lines deriving from single clones, cell suspensions were diluted to contain cell number ranging from 0.01-10 cells per well and plated in a 96 well set up.

DNA isolation

Plasmids were isolated using QIAprep Spin Miniprep Kit (QIAGEN) or QIAGEN Plasmid Maxi Kit (25) (QIAGEN) following manufacturer's instructions. To extract DNA from cell lines, 1×10^6 cells were washed in PBS twice before lysing in 1ml Quick Tail Lysis Buffer (0.1% (w/v) SDS; 10 mM Tris-Cl pH 8.0; 1 mM EDTA pH 8.0; 5 mg/ml DNase-free RNaseA; 5 M Potassium acetate; 20 µg/ml Proteinase K) at 55°C for 3 hours. Proteinase K was subsequently inhibited by keeping the lysate at 99°C for 20 minutes. Samples were amplified by PCR, analyzed on an agarose gel and subjected to sanger sequencing

LDH release assay

5×10^5 THP1 cells were seeded in 96 well tissue culture treated plates in 100µl RPMI 10% FBS µg/ml P/S 80nm PMA 72 hours prior to treatment. Media was exchanged to RPMI 10% FBS µg/ml P/S substituted with VBP or DMSO control as indicated, in triplicate. To assay drug cytotoxicity in myeloid mouse cell lines or BMDMs, 1×10^5 cells were seeded in 100 µl DMEM 10% FBS 100 µg/ml P/S + 200 nM Glutamate 2 h before treatment. LDH release was assayed with Pierce LDH Cytotoxicity Assay Kit (Thermo Scientific), according to manufacturer's instructions. LDH release was calculated with the following formula

$$\% \text{ Cytotoxicity} = \frac{\text{Compound-treated LDH activity} - \text{Spontaneous LDH activity}}{\text{Maximum LDH activity} - \text{Spontaneous LDH activity}} \times 100$$

whereby cells treated with lysis buffer were taken as reference for 100% toxicity and samples were normalized to vehicle control (DMSO).

Protein Isolation

Whole cell protein was isolated by lysing the cells in NP-40 Lysis buffer (2 mM EDTA, 1% Nonident P-40, 20 mM Tris/HCl pH8, 10% Glycerol, 137mM NaCl; protease inhibitor (cOmplete Tablets, Roche), 1 mM PMSF, 1mM Sodium Orthovanadate), and subsequent incubation (rotating) at 4°C for 30 minutes. Cell debris was pelleted by centrifugation at 21000 g for 10 minutes at 4°C and protein concentration of the supernatant quantified with DCTM Protein Assay (BIO-RAD).

SDS Polyacrylamide Gel electrophoresis and Western blot analysis

Protein Samples were separated on a 4-12% Bis-Tris Polyacrylamide Gel (Invitrogen, # NP0322BOX) in 1x NuPAGE MOPS SDS Running buffer (Invitrogen, #NP0001) running buffer at 130V. 4 µl Precision Plus Protein Standard (BIO-RAD, # 1610374) were loaded as reference. Protein was transferred onto methanol activated polyvinylidene fluoride (PVDF) membrane, equilibrated in 1x NuPAGE Transfer Buffer (Invitrogen) with 10% methanol. The transfer was conducted as wet transfer for 2 h at 120 V at 4°C. Subsequently, the PVDF membrane was blocked in 5% milk solution in TBS-T (25 mM Tris, 0.15M NaCl, 0.05% Tween-20, pH 7.5) for a minimum of 15 minutes prior to incubation with the primary detection antibody. Antibodies were dissolved in TBS-T (concentration indicated in Table 4) and incubated 1 hour on a tilting shaker (RT).

Table 4 Antibodies for Western blot detection

| Reagent or Resource | Source | Identifier | Working Dilution |
|--|----------------|---|------------------|
| rabbit α- DPP9 | Abcam | Anti-DPP9 antibody - Catalytic domain (ab42080) | 1:5000 |
| rabbit α- ASC | AdipoGen | anti-Asc, pAb (AL177) (ATTO 647N) | 1:1000 |
| sheep α- NLRP1 | R&D Systems | Human NLRP1/NALP1 Antibody (AF6788-sp) | 1:80 |
| rabbit α-CASP-1 | Cell signaling | Human CASP1 (#2225) | 1:1000 |
| goat α- Actin | Santa- Cruz | Actin (I-19) sc-1616 | 1:300 |
| α- mCasp1 | adpiogen | Casper-1 | 1:1000 |
| α- IL-1β | Cell signaling | IL-1 β (D4T2D) Rabbit mAB #12426 | 1:1000 |
| α- β-Tubulin | DSHB | E7 | 1:5000 |
| Streptavidin-HRP | R&D Systems | Part No. 893975 | 1:1000 |

The PVDF membrane was washed additional 3 times with TBS-T and incubated with appropriate secondary antibody conjugated to horseradish peroxidase (HRP) in TBS-T for 1 hour on a tilting shaker. West Pico PLUS Chemiluminescent Substrate (Super Signal™, Thermo Fisher Scientific) was detected on X-ray film.

DPP activity assay

Cells were washed twice in ice cold PBS and once in DPP activity assay buffer (20 mM Tris/HCl pH 7.5, 500 mM sodium chloride, 1mM DTT). Cells were homogenized with polytron PT 2100 homogenizer (KINEMATICA; Lucern, Schweiz) and protein was quantified with DC™ Protein Assay (BIO-RAD). Lysates were incubated with inhibitors as indicated in the result section. Gly-Pro p-nitroanilide hydrochloride (H-Gly-Pro-pNA; SIGMA, #G0513) to a final concentration of 1mM was added and accumulation of the chromogenic substrate p-nitroanilide was assayed every 10 minutes by measuring absorbance at 405 nm while incubating at 37°C utilizing SYNERGY HTX multi-mode reader (BioTek Instruments; Winooski, USA).

Speck formation Microscopy

To assay Speck formation in mBMDMs, cells were seeded in glass bottom plates and fixed by adding equal volume of ice cold MetOH directly to culture media and incubating for 30 min at 20°C. Fixed cells were washed twice with PBS and blocked in PBS containing 2% BSA and 0.3% Triton for 30 min at room temperature. Primary antibodies were diluted in PBS with PBS containing 1% BSA and 0.1% Triton overnight at 4 degrees C. Wells were washed twice in PBS and incubated 1 hour covered from light with secondary antibody cocktail, containing according secondary antibody together with DAPI (1:1000; Sigma-Aldrich, D9542) and Phalloidin CruzFluor™ 647 Conjugate (1:500; Santa Cruz Biotechnology sc-363797). Images were acquired with Leica DMI6000B inverted microscope and data was analyzed using the LAS-AF software.

Statistical analysis

Statistical Analysis was conducted with GraphPad Prism version 7.0a for Mac (GraphPad Software, La Jolla California USA, www.graphpad.com). Statistical significance was assessed by Student's t test or two-way ANOVA as indicated, whereby a p value < 0.05 was considered as statistically significant.

Results and Discussion

Nlrp1 is the responsive sensor for Valboro-Pro induced pyroptosis in mBMDMs

Valboro-Pro, an immunomodulatory drug, induces pyroptosis in RAW264.7 cells via activation of pro-caspase-1 and cleavage of its substrate GSDMD.^[10] Classic caspase-1 activation requires CARD mediated association with the adaptor protein ASC in order to form large multimeric complexes that allow autoproteolytic cleavage for the activation of caspase-1.^[38, 47] ASC proteins assemble to specks that form in response to inflammasome sensor activation. Multi-protein association of inflammasome sensors provides oligomerization platforms for ASC via PYD domains.^[38] RAW264.7 cells, a murine-leukemic monocyte-macrophage cell line, do not express the adaptor protein ASC^[83]. In addition, THP1 cells lacking ASC maintain their responsiveness to VBP^[10]. Therefore, caspase-1 activation following VBP treatment occurs independently of ASC. To test this hypothesis, we generated mouse bone marrow derived macrophages (mBMDMs) of ASC knockout (*Asc*^{-/-}) mice and determined their responsiveness to VBP (Figure 5A). The cells were treated with 25µM VBP for 24 hours. The pyroptotic effects of VBP on mBMDMs were assayed by quantifying the release of LDH into the medium, indicating disruption of the plasma membrane.^[90, 91] *Asc*^{-/-} mBMDMs displayed an intermediate responsiveness to VBP compared to WT or *Casp1*^{-/-} mBMDMs (Figure 5A).

Caspase-1 activation happens downstream of inflammasome sensor oligomerization.^[38] The only known inflammasome sensors that are able to interact directly with caspase-1 are *Nlrp1* and *Nlrc4*.^[38, 53] These sensors possess an endogenous CARD domain, allowing for direct CARD-CARD interaction.^[38, 55] Preliminary data of the Flavell Lab showed that mBMDMs derived from *Nlrc4*^{-/-} mice displayed the same responsiveness to VBP as WT (Figure 4). To determine whether *Nlrp1* senses VBP induced DPP8/9 inhibition and therefore mediates pyroptosis, mBMDMs of *Nlrp1*^{-/-} mice were generated and treated with 25µM VBP for 24 hours. *Nlrp1*^{-/-} mice were generated on a 129 background, targeting exon 1-3 of the *Nlrp1b* gene.^[84] The genome of 129 mice encodes for functional *Nlrp1b* while *Nlrp1a* and *Nlrp1c* are non-functional, resulting in complete loss of *Nlrp1* function in this strain.^[84] *Nlrp1*^{-/-} mice were subsequently backcrossed to C57BL/6J, to generate a line congenic for the *Nlrp1* locus.^[84] Sensitiveness to VBP was assayed by detecting the leakage of

LDH into the supernatant. Our experiments showed that *Nlrp1*^{-/-} mBMDMs are resistant to VBP treatment, indicating *Nlrp1* and not *Nlrp4* is the inflammasome sensor mediating VBP induced pyroptosis (Figure 5).

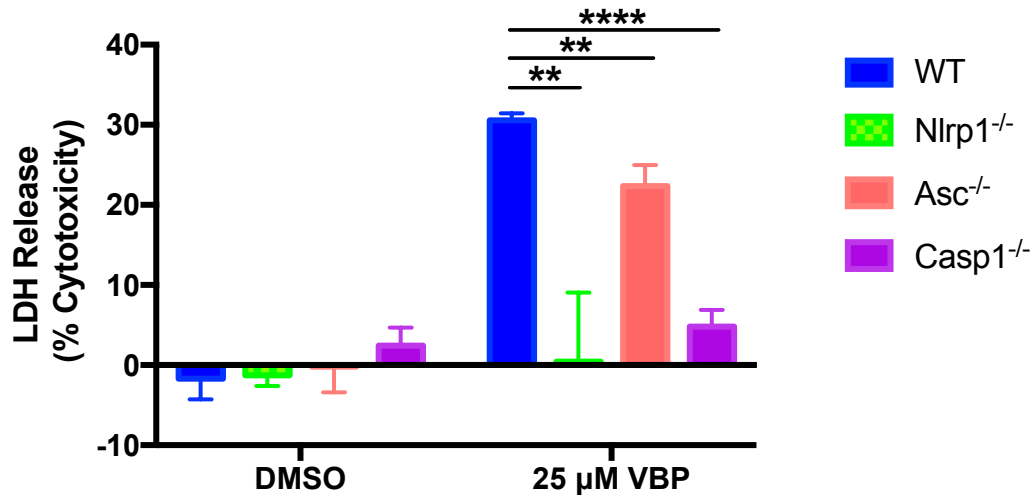


Figure 5 *Nlrp1* is the responsive sensor for VBP induced pyroptosis in mBMDMs. mBMDMs were generated from mice of indicated genotypes and treated with 25μM VBP for 24h. LDH leakage was assayed to estimate lytic cell death. ****p<0.0005, **p<0.005

Upon activation, *Nlrp1* oligomerizes and recruits ASC to form a multiprotein complex, able to interact with caspase-1, leading to its processing and activation.^[38] To complement our findings, we performed immunofluorescence on *Nlrp1*^{-/-} mBMDMs to determine ASC speck formation. Cells were seeded in a glass bottom 24 well and treated with 25μM VBP for 24 hours or 5 hours with 100ng/ml LPS plus 15 min 10μM Nigericin prior to fixation and staining. ASC and Casp-1 were fluorescently labelled, *Asc*^{-/-} and *Casp-1*^{-/-} mBMDMs were used as control. The strong yellow signals detected in WT cells treated with VBP or LPS/Nigericin indicate highly concentrated colocalization of ASC and Casp-1 specks, demonstrating that WT cells form ASC/caspase-1 specks upon VBP treatment (24h, Figure 6A). No ASC-caspase-1 specks were detectable in *Asc*^{-/-} treated with either VBP or the positive control LPS/Nigericin, thereby validating the specificity of the antibody. Formation of ASC specks in response to VBP treatment was not impaired by the lack of Casp-1, as this protease is recruited post ASC assembly. *Nlrp1*^{-/-} mBMDMs did not form ASC specks upon VBP stimulation (Figure 6A, B). To the best of our knowledge, no knockout-validated *Nlrp1* specific antibodies exist that could be used to directly detect *Nlrp1* association to the observed ASC specks. However, combining cell death assay and immunofluorescence, these data show that *Nlrp1* mediates VBP induced lytic cell death.

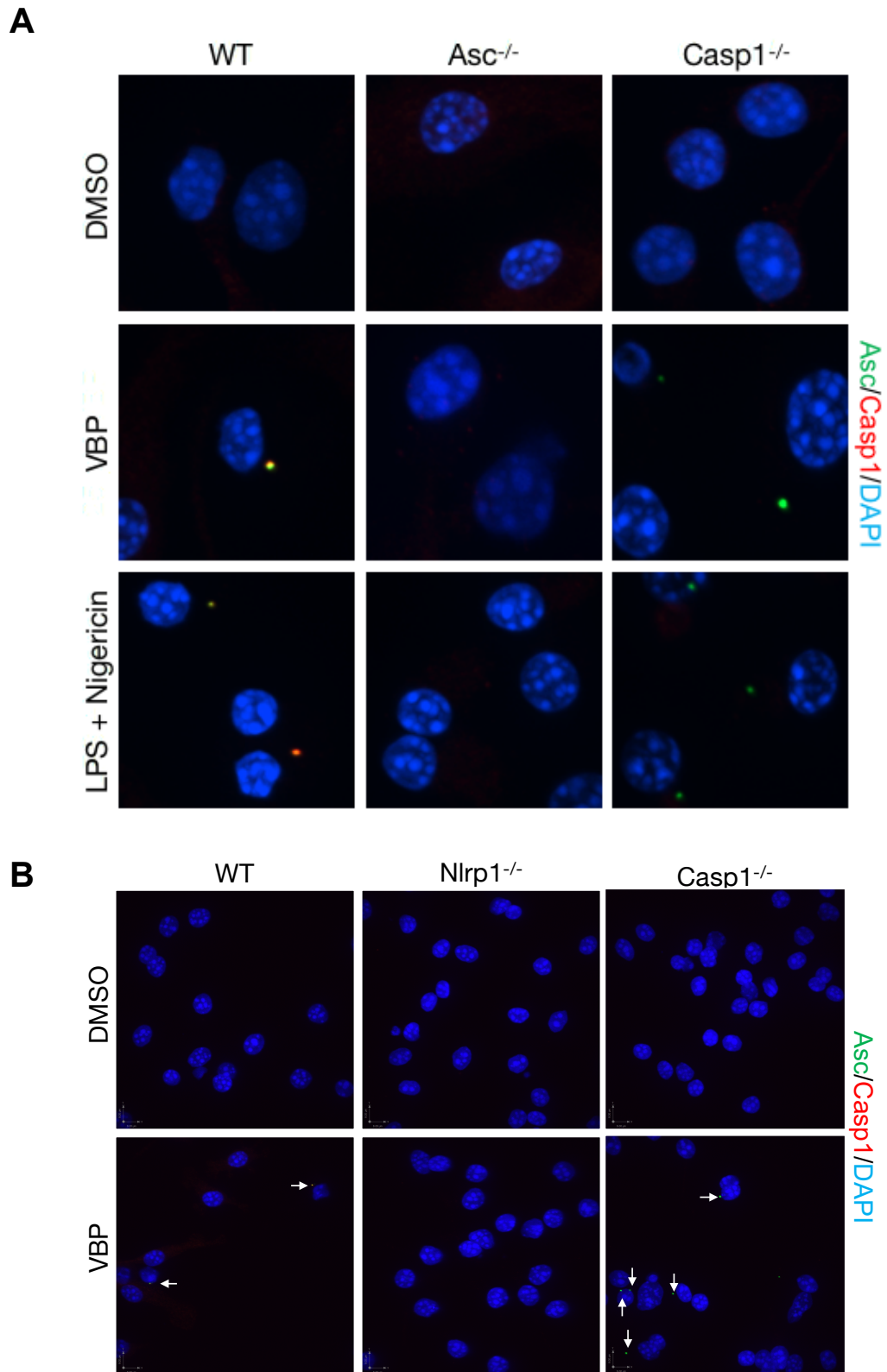


Figure 6 Immunofluorescent staining of ASC and Caspase Speck formation. Cells were seeded in a glass bottom 24 well and treated with 25 μ M VBP for 24 hours or 5 hours with 100ng/ml LPS plus 15 min 10 μ M Nigericin, respectively. A) VBP induces ASC and caspase-1 speck formation in WT cells. Yellow fluorescence indicates colocalisation. B) VBP induced ASC speck formation in WT and caspase-1 knockouts but not Nlrp1^{-/-}. Images were taken and kindly provided by James Richard Brewer.

Cleavage of caspase-1 upon inflammasome activation can be detected via western blot analysis of its autoproteolytic cleavage products p20 and p10 that form heterodimers to process their substrates such as IL-1 β and IL-18.^[38, 48, 49] Stimulation with VBP did not lead to the expected autoproteolytic cleavage of caspase-1 (Figure 7A) as no p20 product was detected. However, stimulation with LPS and Nigericin lead to cleavage of caspase-1. Complementing our findings, Okondo et al 2017 were likewise not able to detect p20 cleavage products. Despite the lack of detectable p20 elements upon VBP treatment, caspase-1 might still be able to cleave its substrates. In addition to our data and Okondo's et al. 2017, that identify caspase-1 as effector molecule responsible for VBP's induction of pyroptosis, others report that caspase-1 mutants deficient for auto-cleavage are still able to induce cell death.^[48, 50, 55] In the same studies, ASC knockout mice are shown to be sensitive to the anthrax lethal toxin. Van Opdenbosh et al. provide evidence for Nlrp1 and caspase-1 activation independent of ASC, further supporting our hypothesis that ASC is dispensable for VBP mediated inflammasome activation and induction of pyroptosis.^[55]

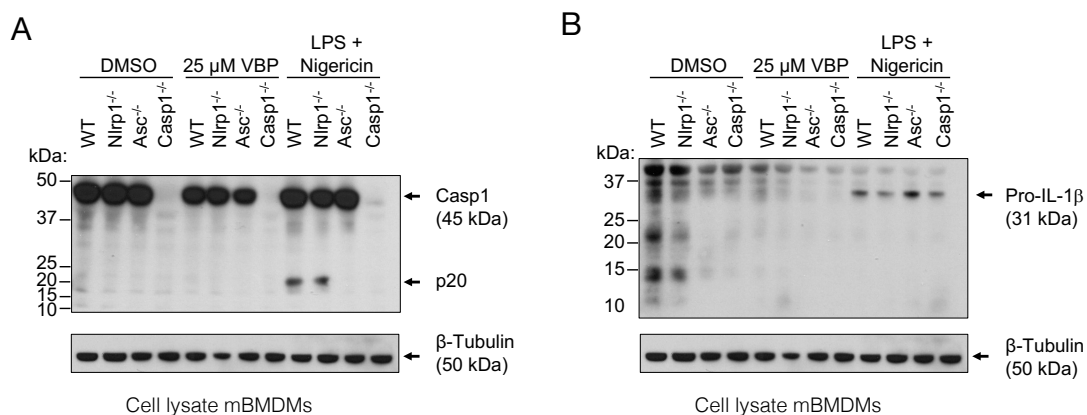


Figure 7 Western blot detection of Casp-1 and pro-IL-1 β . mBMDMs were stimulated for 24h with 25 μ M VBP or 100ng/ml LPS and 10 μ M Nigericin, respectively. A) Detection of pro-caspase-1 and p20 cleavage product. B) detection of IL-1 β (pro-IL-1 β and mature IL-1 β are distinguishable via their size).

To detect whether VBP also changes the abundance of pro-IL-1 β in the cytosol of sensitive cells, we performed western blot analysis of mBMDMs after stimulation for 24h with 25 μ M VBP. Stimulation with 100ng/ml LPS and 10 μ M Nigericin lead to the accumulation of pro-IL-1 β , whereas VBP did not (Figure 7B). Release of mature IL-1 β requires two distinct steps. First, the cell has to receive a stimulus (signal 1) in order

to transcribe and produce pro-IL-1 β . Upon a second signal (signal 2), mature IL-1 β is generated through cleavage of pro-IL-1 β by caspases.^[92] These results indicate, that VBP might not activate signal 1 which induces the transcription of IL-1 β and leads to the accumulation of pro-IL-1 β , but rather signal 2, inducing cleavage and maturation of IL-1 β , IL-18 and the death effector protein GSDMD.^[47]

Valboro-Pro does not alter tumor growth in EL4 cancer models

VBP is an immunomodulatory drug, restricting tumor growth in a T-cell dependent manner.^[80, 82] To test whether the anti-tumor properties of VBP depend on activation of the inflammasome, we decided to exploit the syngeneic EL4 tumor model described by Adams et al. 2004.^[82] Therefore, we injected 500 thousand (k) cells subcutaneously into age matched female C57BL/6 mice (Figure 8A; experimental setup). Starting on day 2, mice were treated twice daily p. o. with 20 μ g VBP, at 8 hour intervals, over the course of eleven days. Despite the significant findings of Adams et al., no differences of EL4 tumor growth in C57BL/6J mice were detected (Figure 8).

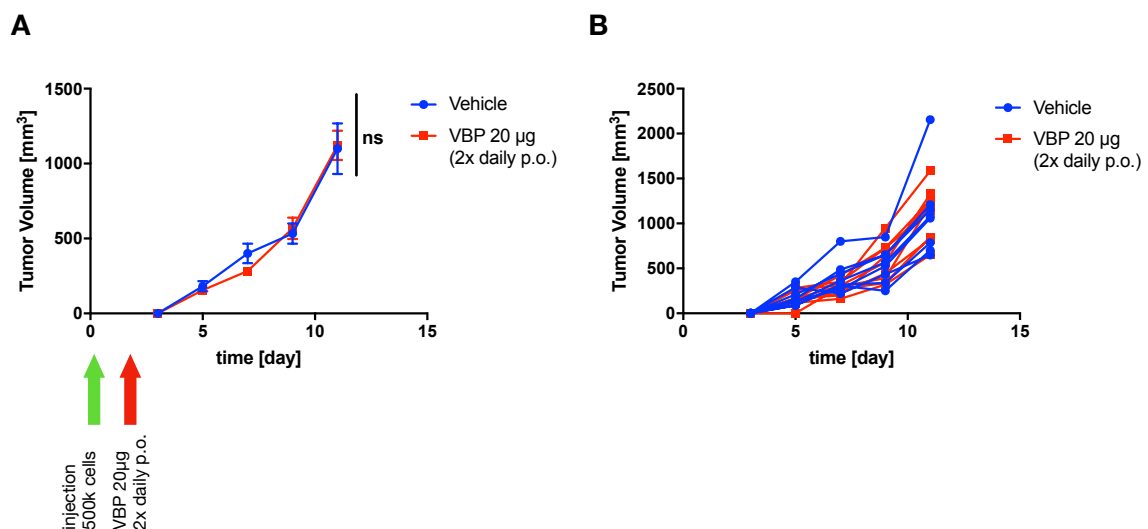


Figure 8 VBP does not attenuate tumor growth in EL4 syngeneic tumor model. Mice were treated twice daily with 20 μ g VBP, tumor volumes were assayed with a caliper, measuring 2 dimensions, serum was collected for further analysis. A) average tumor growth curves (bars indicate SEM). B) Tumor growth curves of individual mice; statistical significance of differences in growth curves was assayed with 2-way-ANOVA.

As an internal control, blood was collected to assay for changes in serum cytokine levels. IL-1 β and IL-18 are the main cytokine substrates of caspase-1,^[39, 42] therefore,

we decided to test for changes in serum circulating IL-1 β and IL-18 by ELISA. Other studies reported elevation of CXCL1 in the blood of mice after VBP treatment.^[82] Consequently, we additionally investigated CXCL1 serum levels, a chemokine and attractant for neutrophils.^[93] Administration of VBP gave a 4-fold increase in, but did not significantly alter IL-1 β or Cxcl1 serum levels (Figure 9A). Although others reported Cxcl1 elevation in serum after treatment with VBP^[9], we were not able to detect significant differences.

Different doses of VBP administration might result in differences in Cxcl1 serum levels. Adams et al. 2004 reportedly administered 5 μ g VBP twice daily to the cohort of mice assayed for cytokine levels. In contrast, we administered 20 μ g VBP twice a day. Adams et al stated administration of 20 μ g VBP twice daily as their optimal dosing for their tumor growth studies.^[9] Given the rationale that higher drug doses should increase the observed effects on cytokine concentrations, it is counterintuitive that no differences in Cxcl1 levels were observed. Collecting blood samples at earlier timepoints might display differences in cytokine levels. Notably, the failure of VBP to induce Cxcl1 increase in serum might be the reason why no differences in tumor growth were observed.

Neutrophils are considered to be the first immune cells that are recruited to inflamed tissue^[44]. In addition, neutrophils display anti-tumorigenic properties in early phases of tumor growth by releasing pro-inflammatory cytokines like TNF- α and IL-6.^[26, 94] Moreover, lack of neutrophils has been shown to be indispensable for effective tumor immunotherapy in bladder cancer.^[95] If neutrophil recruitment is essential for VBP mediated tumor growth reduction, neutrophil trafficking and abundance in tumor tissues could be assayed via flow cytometry. Additionally, alterations of other neutrophil chemoattractants upon VBP treatment could be investigated.

Adams et al 2004 did not assay IL-18 or IL-1 β serum levels. IL-1 β is a potent pro-inflammatory cytokine, known to activate macrophages and trigger local and systemic inflammatory responses of the immune system.^[39, 96] Strong elevation of IL-1 β in serum over a period of multiple days would have severe effects on the whole organism, possibly resulting in metabolic syndromes, chronic inflammation and tissue damage.^[92] For example, overexpression of IL-1 β in the articular of rabbit joints induces systemic inflammation manifested in fever and diarrhea.^[97] These systemic effects were observed in addition to local inflammation resulting in erosion of articular cartilage and

bone. This emphasizes that IL-1 β functions strongly in paracrine fashion. In addition, IL-1 β secretion and high serum levels are found in patients with septic shock or treated with LPS.^[98] Considering its potency, it is not surprising that we were not able to detect differences in IL-1 β serum levels as we would expect to see more severe inflammatory phenotypes in our mice. Accordingly, others, studying the phenotype of a gain of function mutation in the Nlrp1a allele of mice were not able to even detect IL-1 β , despite a clear inflammatory phenotype (pneumonitis, meningitis and hepatitis), assuming its concentration below the detection limit.^[46] Nevertheless, IL-1 β could be elevated locally, at specific sites of inflammation induced by VBP. This hypothesis was further tested by assaying cytokine levels in specific tissue of interest and is discussed in the following chapters. In comparison to IL-1 β , IL-18 is not only reported as pro-inflammatory cytokine but has also been reported to have immunoregulatory effects that actively dampen a pro-inflammatory response.^[20, 46] Masters et al. 2012 demonstrated, that gain of function Nlrp1a mice lacking IL-18, displayed higher numbers of neutrophils in the blood and the onset of the inflammation observed was strongly accelerated.^[46]

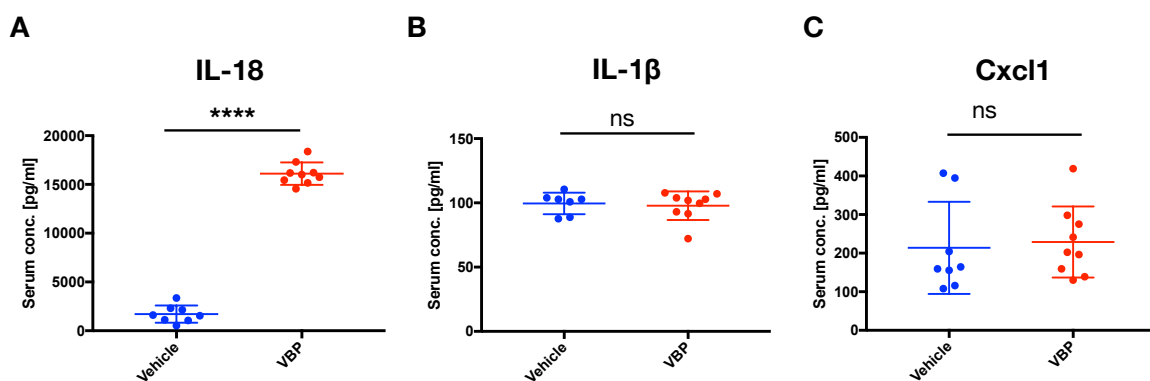


Figure 9 VBP effects on cytokine levels in serum. Serum was collected of mice treated with vehicle control or VBP for 11 days. Cytokine levels of A) IL-18, B) IL-1 β and C) Cxcl1 were assayed with ELISA. Statistical significance was assayed with unpaired t-test. **** $p < 0.0005$.

It is important to point out that we performed our experiments in C57BL/6J mice. EL4 cells are syngeneic to C57BL/6N. Different backgrounds can lead to unpredictable differences in immunological studies.^[99, 100] Adams et al. 2004 executed their experiments in C57LB/6 mice, but does not indicate whether the WT strains used are of the subtype N or J. Testing different C57BL/6 population alone could be the reason for not replicating Adams' et al. 2004 results. Therefore, we carefully controlled for background effects in all subsequent conducted tumor studies.

Given that we were not able to see differences in tumor growth between VBP and vehicle treated cohorts with the EL4 cell line, we decided to exploit additional cancer models to establish a solid system to address the question whether VBP's published anti-tumor effects depend on Nlrp1 and caspase-1.

VBP mediates tumor growth suppression in syngeneic MC38 and YUMMER1.7 cancer models

Immunotherapy as cancer treatment was poorly investigated by the time VBP was first tested for its tumoricidal properties.^[101, 102] Considering the immunomodulatory potential of VBP, we decided to assay its anti-tumor effects with a cell line that has been shown previously to respond to immunotherapy-drugs like Nivolumab (anti-PD-1) and Ipilimumab (anti-CTLA4).^[6] The murine colorectal cancer cell line MC38 is responsive to immunotherapy, blocking the PD-1/PD-L1 pathway.^[7] Utilizing this cancer cell line, we are able to show that administration of VBP leads to significant tumor growth restriction in WT mice compared to vehicle control (Figure 10).

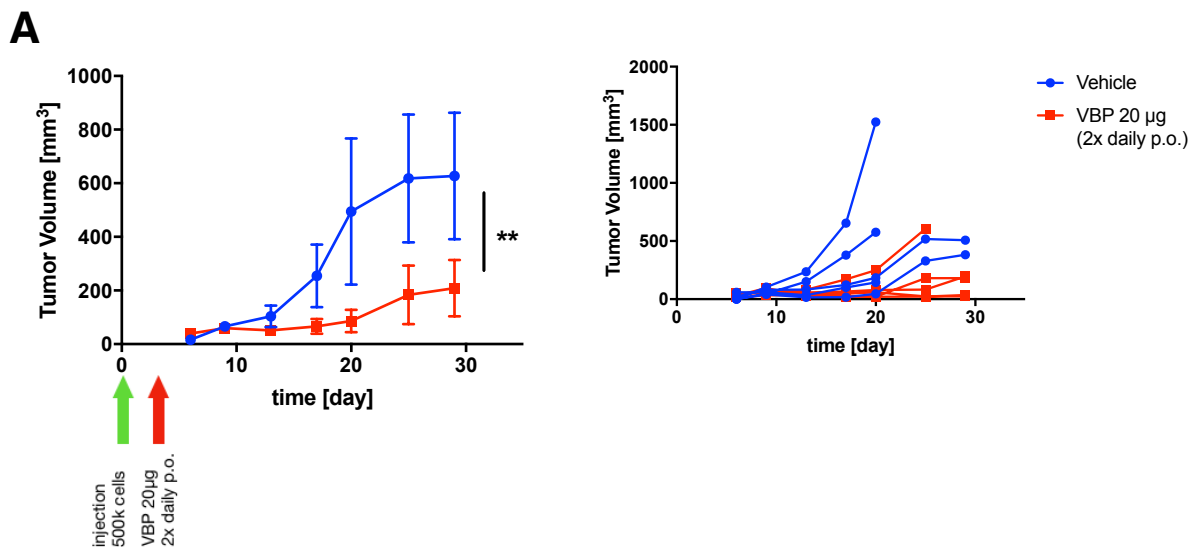


Figure 10 VBP attenuates tumor growth in MC38 model. 500k MC38 cells were injected subcutaneously. Mice were treated with 20µg VBP or vehicle control twice daily p.o. starting on day 2 A) average of tumor growth curves of WT mice treated with VBP or vehicle control (error bars indicate SEM; significance was assayed with 2-way-ANOVA). B) plot of individual growth curves. **p<0.005

Due to their susceptibility to immune checkpoint inhibitors, we additionally utilized the C57BL/6 syngeneic YUMMER1.7 and YUMMER1.7-GFP line.^[87, 103]

In the YUMMER1.7-GFP model, VBP administration lead to tumor growth suppression in all treated mice (Figure 11). Tumors of two of the mice treated with the vehicle control

regressed spontaneously, leading to a final tumor incidence of 60% compared to 0% in the VBP cohort at the end of the experiment, respectively (Figure 11B).

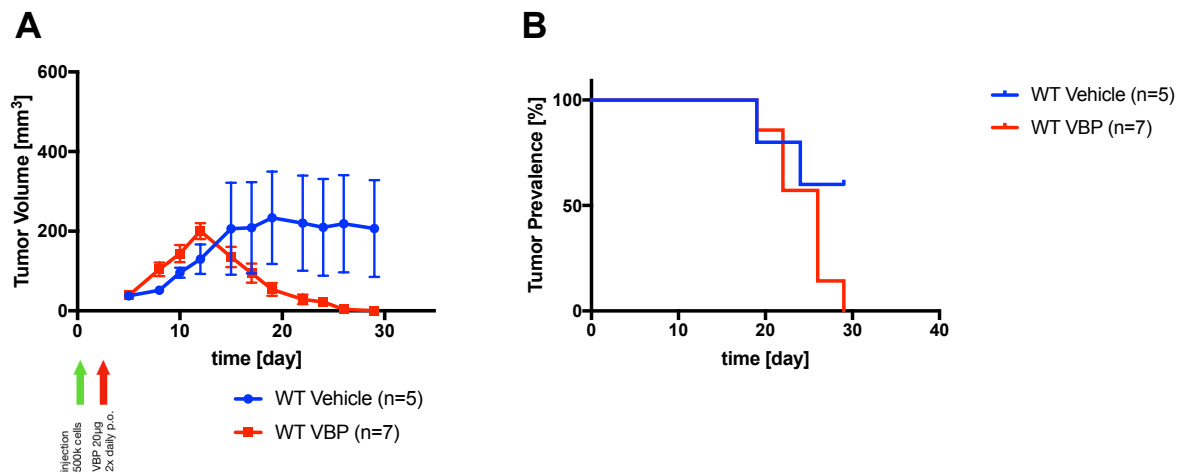


Figure 11 VBP attenuates tumor growth in YUMMER1.7-GFP model. 500k cells were injected subcutaneously. Mice were treated with 20µg VBP or vehicle control twice daily p.o. starting on day2. A) average of tumor growth curves of WT mice treated with VBP or vehicle control (error bars indicate SEM; significance was assayed with 2-way-ANOVA). B) Kaplan-Meier-Graph displaying tumor prevalence (right). *p <0.05

If injected with 100k YUMMER1.7 cells, spontaneous T cell dependent rejection of melanomas was previously reported in C57BL/6J, while injection of higher cell numbers (~250k-1000k) overcomes this regression.^[87] According to the authors, Injection with 500k cells should result in exponentially growing tumors.^[87] Given the occurrence of spontaneous rejection in WT mice treated with the vehicle control with initial injection number of 500k cells, we hypothesized that the transgene GFP might act as neoantigen, despite previous published observations.^[87, 103] To circumvent this possible disadvantage, we performed our next study utilizing YUMMER1.7 that do not express GFP.

Oral administration of VBP lead to a clear decrease in tumor volume in WT mice compared to the vehicle treated control group (Figure 12A). 78% of tumors in WT VBP treated mice regressed completely over the course of the experiment (Figure 12B). All vehicle treated WT mice still bared tumors on day 34 (Figure 12B).

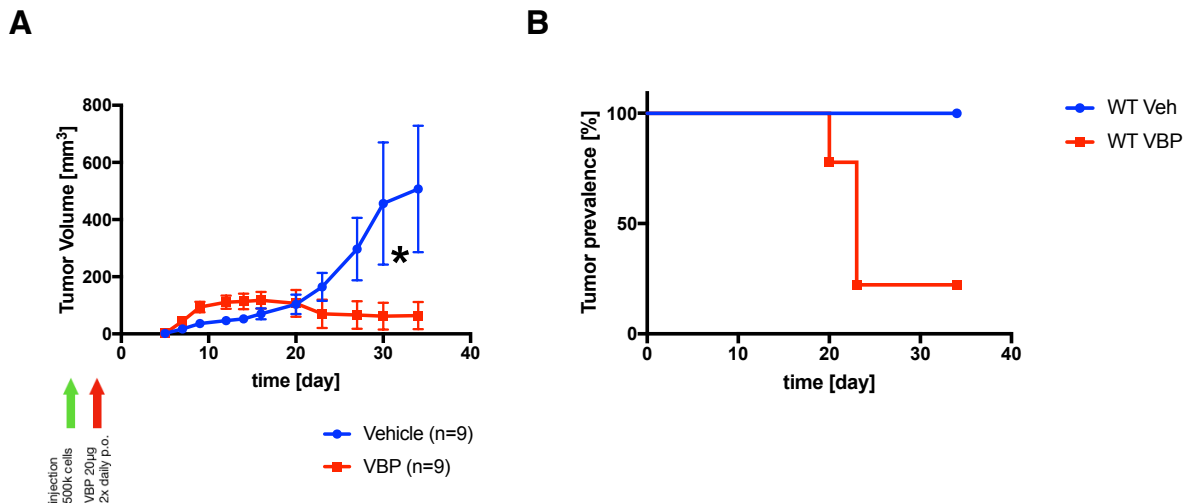


Figure 12 VBP causes tumor regression in YUMMER1.7 cancer model. 500k cells were injected subcutaneously. Mice were treated with 20µg VBP or vehicle control twice daily p.o. starting on day2. A) average of tumor growth curves of WT mice treated with VBP or vehicle control (error bars indicate SEM; *p <0.05, significance was assayed with 2-way-ANOVA). B) Kaplan-Meier-Graph displaying tumor prevalence (right, tumors that never exceeded a total volume of 15mm³ are excluded of the Kaplan-Meier-Plot).

In addition, we excluded direct cytotoxicity of VBP on YUMMER1.7 cells by assaying LDH release upon VBP treatment in vitro. YUMMER1.7 cells were not responsive to VBP.

Figure 13 VBP does not directly induce pyroptosis in YUMMER1.7 cells. A) LDH release assay of VBP responsive GFP-THP1 cells in comparison to YUMMER1.7; cells were treated with 100µM VBP for 24h. Statistical significance was assayed with Student's t-test. ****p<0.0005

Valboro-Pro induced pyroptosis in THP1 cells is dependent on Caspase1

To determine, whether VBP induce inflammasome activation and pyroptosis in human cells, we aimed to generate THP1 knockout cell lines of DPP9, Nlrp1, ASC and caspase-1. Therefore, the lentiCRISPRv2 system constructed by Feng Zhang was exploited.^[88] Genes of interest were targeted with a single guide, resulting in a directed cleavage event mediated by the nuclease Cas9.^[104] The resulting double strand break is subsequently repaired by the non-homologous end joining (NHEJ) repair pathway, either reconstituting the WT allele or resulting in indels. These insertions or deletions regularly lead to frameshift mutations inserting a premature stop codon in the open reading frame. Hence, loss of protein can be detected via western blot. Utilizing this method, we successfully generated DPP9 and ASC knockouts (Figure 14).

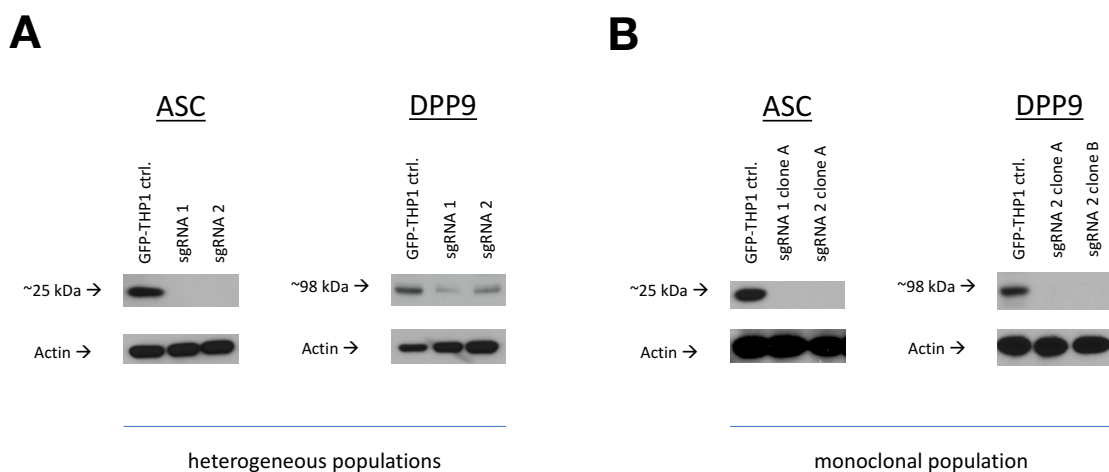


Figure 14 THP1 ASC and DPP9 knockouts. A) western blot of heterogeneous ASC and DPP9 knockouts after lentivirus transduction. B) western blot of ASC and DPP9 knockout cell lines after monoclonal expansion. sgRNA indicates guide RNA sequence used to knock out GOI.

Western blot detection of the heterogeneous THP1 populations after virus transfection showed reduction of DPP9 and complete loss of ASC protein compared to THP1 control cells (THP1-GFP, Figure 14A). THP1-GFP cells were transduced at the same time with a lentiGFP construct and are therefore stably expressing GFP. ASC^{-/-} and DPP9^{-/-} THP1 cell lines were subsequently derived from a single clone. After expansion of those single-cell derived clonal cell lines, knockout was reconfirmed by western blot (Figure 14B).

We were not able to determine Nlrp1 and caspase-1 knockout via western blot. In our hands, various antibodies previously published did not show sufficient specificity (representative blot shown in Figure 15A). The antibodies tested were not validated by

knockouts in previous studies, and detected multiple unspecific bands in our experiments. Hence, the results were inconclusive. To complement the outcome of the western blot analysis, we chose LDH release as our functional readout. Leakage of LDH into the supernatant upon VBP treatment indicates pyroptosis of THP1 cells.^[10, 90] Monoclonal cell lines derived from Casp1^{-/-} population displayed resistance to VBP mediated LDH release compared to WT THP1 (Figure 15B). These results indicate that despite uninterpretable western blot results, these clones do not possess functional caspase-1. Consequently, we topo-cloned the locus of interest to separate the two alleles and sequenced Casp1^{-/-} clone B. Sanger sequencing and alignment with WT reference sequence confirmed the deletion of 16 base pairs leading to the incorporation of a premature stop codon (Figure 15C). The sequencing results together with the functional readout confirm the knockout of caspase-1 in the CASP1^{-/-} B clone line (targeted by sgRNA 2).

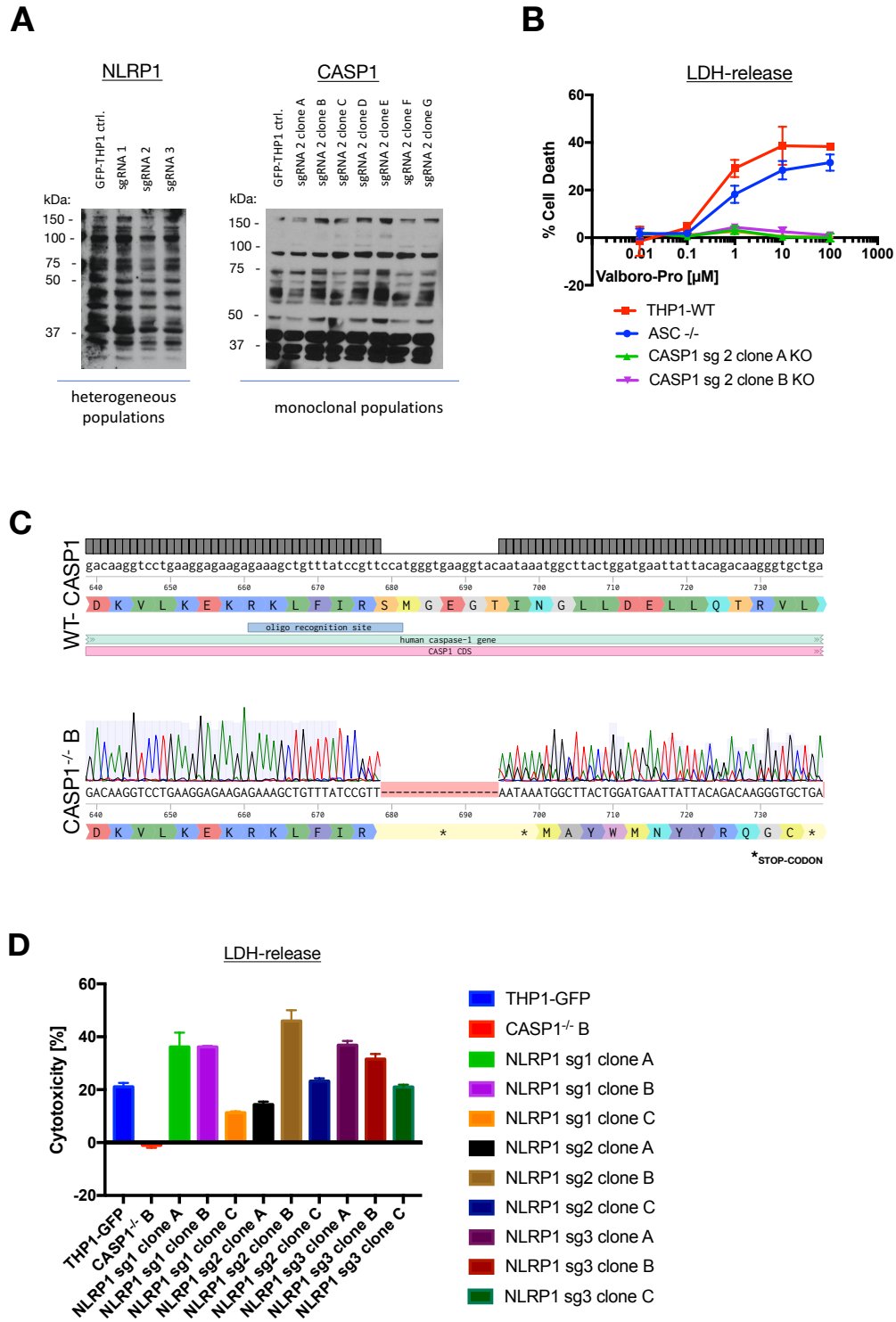


Figure 15 Validation of THP1 knockouts of inflammasome components. A) representative images of failed knockout confirmation of NLRP1 and CASP1. B) LDH release assay of THP1 inflammasome knockout clones compared to WT THP1. C) sequence alignment of human WT caspase-1 gene (NHI RefSeq CM000673.2) and sgRNA 2 targeted $CASP1^{-/-}$ clone B. D) LDH release assay of NLRP1 $^{-/-}$ clones.

LDH release performed with multiple Nlrp1^{-/-} clones gave ambiguous results. No clear loss of VBP sensitivity can be concluded (Figure 15D). Together with the inconclusive western blot data, this does not reveal whether pyroptosis as response to VBP treatment happens independently of Nlrp1 in THP1 cells or if the knockout strategy was unsuccessful. It is likely, that we were not able to successfully knockout Nlrp1. To be able to determine a knockout on the DNA or transcriptional level, we aimed to exploit a two-guide strategy of the lentiCRISPRv2 system. This would introduce 2 guides simultaneously into the cell. We targeted exon one and four; loss of those would result in a frameshift. Therefore, these knockouts could be validated by qPCR. However, in the course of our studies, others published Nlrp1 independent pyroptosis in THP1 cells upon VBP treatment.^[105] Johnson et al. 2018 showed that VBP induced pyroptosis in THP-1 and MV4;11 Nlrp1^{-/-}, demonstrating that Nlrp1 is not the responsible sensor for mediating VBP induced cell death in those cell lines.^[105] These results affirm our results of the LDH release, under the assumption that we did generate knockouts, albeit unsuccessful in validating Nlrp1^{-/-}.

Given our positive results in the tumor experiments we therefore decided to further investigate VBP's dependence on Nlrp1 in our tumor models and put the generation of Nlrp1^{-/-} THP1 on hold and resume when needed. However, we successfully generated DPP9^{-/-}, ASC^{-/-} and Casp-1^{-/-}. Casp-1^{-/-} were resistant to VBP induced pyroptosis while ASC^{-/-} displayed a minor reduction compared to WT-THP1 cells (Figure 15B).

Valboro-Pro and changes in redox potential inhibit DPP activity in vitro

Dipeptidyl peptidases of the DPP4 family have a specificity for cleaving their substrates after a proline at the penultimate position of the N-terminus, releasing the N-terminal dipeptide.^[75] The intracellular serine proteases DPP8 and DPP9 are involved in protein degradation and cleave molecules with known immunological functions such as IL1-RA or Cxcl10.^[73] Prior publications determined DPP8 and DPP9 as main targets to the inhibition of the boronic acid VBP.^[10] In addition to inhibitory drugs, PAMPs, DAMPs or endogenous signals have the potential to inactivate DPP8 and 9 and initiate inflammasome activation. To be able to measure the activity of DPPs, we utilized the accumulation of the chromogenic product p-nitroanilide (pNA) as a proxy for overall DPP activity. The substrate H-Gly-Pro-p-nitroanilide (H-Gly-Pro-pNA) displays a

proline at the N-terminal penultimate position. DPP4 family members cleave off the N-terminal dipeptide and therefore release the chromogenic part p-nitroanilide. The accumulation of pNA is determined via absorbance measurement at 405nm. Differences absorbance can be used to compare DPP activity between different genotypes (knockouts or mutations of DPP family members) or conditions (inhibitors, treated vs. non-treated).

THP1 cells were differentiated with 80nM PMA for 72 hours. For in vitro DPP activity assay, cells were harvested in DPP activity assay buffer and lysed with a homogenizer. Cell lysates were incubated 5 min with 25 μ M VBP or vehicle control prior to H-Gly-Pro-pNA addition. Accumulation of pNA was assayed by measuring the absorbance at 405nm at 37°C for 2 hours.

The addition of VBP to the cell lysates inhibits the accumulation of pNA as depicted in Figure 16. Lysates of THP1 cells lacking DPP9 displayed less and slower pNA accumulation and compared to WT cells in the vehicle control treated groups (Figure 16A and B, respectively). As expected, this intermediate phenotype indicates that DPP9 is not the only dipeptidyl peptidase capable of cleaving the substrate H-Gly-Pro-pNA. THP1 cells do not express DPP4 or FAP^[10]. Hence, DPP8, the DPP with the greatest similarity to DPP9 and DPP7 are obvious candidates.^[106]

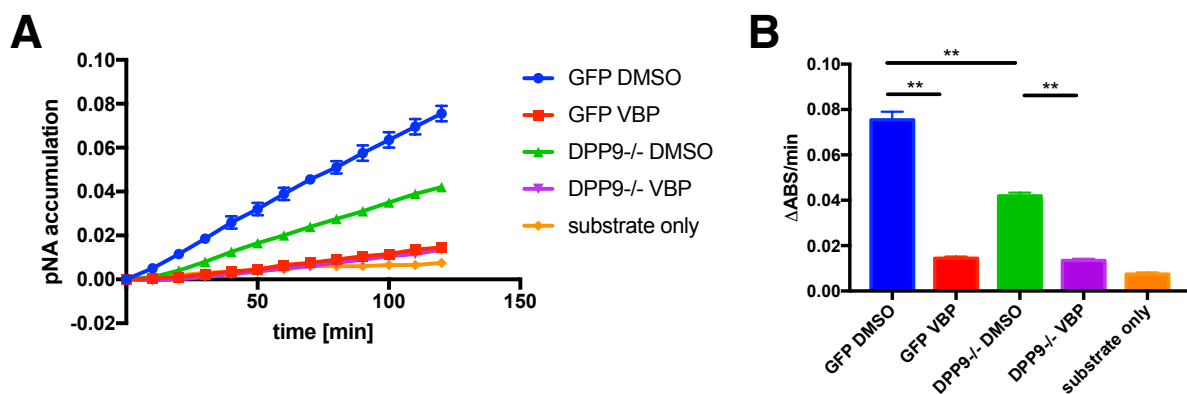


Figure 16 DPP activity assay. THP1 cell lysates were incubated for 2h at 37°C with vehicle control (DMSO) or VBP. A) Monitoring of pNA accumulation over the course of 2 hours. B) Representation of Δ ABS/min as a proxy for DPP activity. Significance was assayed with Student's t-test. ** $p < 0.005$.

Considering the broader range of inhibition of VBP^[10], redundancy of different DPPs explains the further reduction in pNA accumulation upon the addition of VBP. In order to test these hypotheses, double or triple knockouts of named serine proteases or more specific inhibitors of DPP8/9, like 1G244^[10], can be investigated to evaluate which are the main enzymes cleaving the chromogenic substrate. However, this is not the main

focus of these studies. Another approach to investigate changes in activity of DPPs is to utilize a biotinylated fluorophosphonate probe (FP-biotin) that specifically detects serine hydrolases in an activity-dependent manner.^[10, 107] Serine hydrolases interacting with the FP-biotin probe can be purified and classified via western blot.^[107]

Previous studies showed that the activity of DPP8 and DPP9, but not DPP4 is reduced if cysteine residues close to the catalytic center are oxidized.^[75] These studies exploited the bacterial co-enzyme pyrroloquinoline quinone (PQQ) and H₂O₂ and demonstrated their inhibitory effect on DPP8/9 in vitro. We incubated cell lysates with different concentrations of H₂O₂ (2x dilutions; 100-1.5625 μmol/l, respectively) while assaying pNA accumulation. Correspondingly, we were able to show that DPP activity is sensitive to H₂O₂ concentration in a dose dependent manner (Figure 17). Delta absorbance per minute decreases with increased H₂O₂ concentration (Figure 17B). This effect was less severe in DPP9^{-/-} cells.

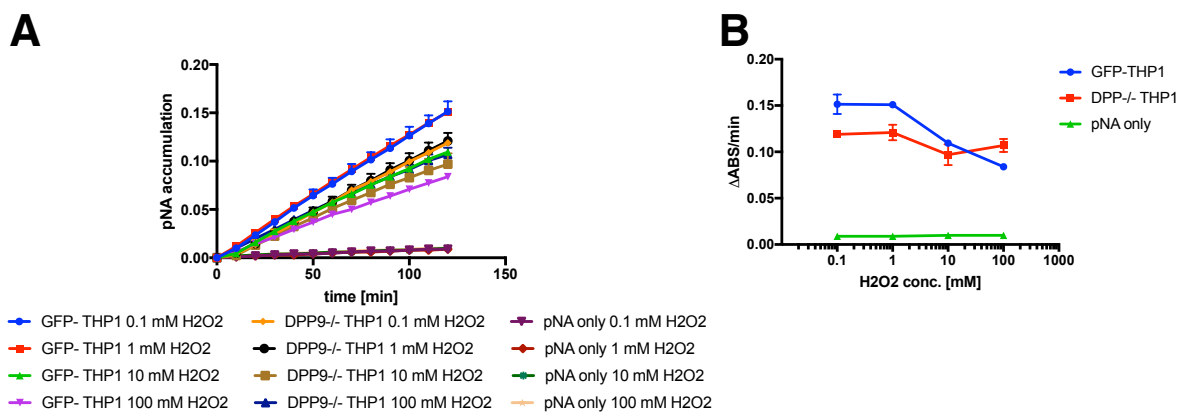


Figure 17 DPPs are sensitive to H₂O₂ concentrations. THP1 cell lysates were treated with increasing doses of H₂O₂ to assay their sensitivity to alterations in redox status. A) Monitoring of pNA accumulation over the course of 2 hours. B) DPP activity shown as ΔABS/min in dependence of H₂O₂ concentration.

H-Gly-Pro-pNA alone was not sensitive to increased H₂O₂ concentrations, supporting that differences observed in the cell lysates occurred due to DPP inhibition rather than spontaneous decay of the substrate. This assay could likewise be revised by utilizing FP-biotin probes to detect changes in activity by western blot rather than accumulation of a chromogenic substrate. Being able to detect changes in the activity of DPPs allows us to investigate how DPPs react to PAMPs, DAMPs or homeostatic alterations in cell lysates. H₂O₂ is released as reactive oxygen species (ROS) into the cytosol as a result of damage or infection.^[108] This could provide important insights in unraveling if and

how DPPs act as sensors to HAMPs and further understand if these mechanisms are likewise linked to the activation of the Nlrp1 inflammasome.

Summary

Cancer immunotherapy revolutionized the treatment of thousands of patients and is stated as the major breakthrough of the last two decades of cancer research.^[5, 6, 15, 28, 109] Some of the most promising recent developments are stimulating the immune system with cytokines (IL-2) and blocking T-cell deactivation by the use of anti-checkpoint inhibitors like Nivolumab (anti-PD-1) and Ipilimumab (anti-CTLA4).^[5, 8, 15, 28, 71] However, not all patients respond to these novel approaches and further research is necessary to unravel new mechanistic targets and improve the efficiency of current treatments. Targeting the innate immune system could enhance current immunotherapies that focus on T cells or reveal novel, independent treatment approaches. Inflammasomes, innate sensors for PAMPs and DAMPs are potent inducers of inflammation and influence tumor growth and metastasis.^[20, 36, 110, 111] In our study, we demonstrated the boronic acid VBP leads to pyroptosis by activating the inflammasome sensor Nlrp1 through a yet unknown mechanism. Furthermore, we provided first evidence, that VBP attenuates tumor growth in syngeneic MC38, YUMMER1.7GFP and YUMMER1.7 cancer models. Investigation of cytokine levels in serum revealed that administration of VBP increases the concentration of IL-18 in circulation

To unravel the mechanistic action of VBP in humans we successfully generated THP1 knockouts of DPP9, ASC and caspase-1. LDH release assay demonstrated that VBP induced pyroptosis is dependent on caspase-1 in THP1 cells. We were not able to validate NLRP1^{-/-} THP1 cells. However, given the published data of Johnson et al. 2018^[105] not NLRP1, but CARD8 mediates pyroptotic cell death in THP1 cells upon VBP treatment. In addition, we showed DPPs in the lysate of THP1 cells have reduced activity if treated with increasing concentrations of reactive oxygen species. These results indicate DPPs as possible sensors for homeostasis-altering molecular pathways (HAMPs).

Outlook and future prospective

As evidenced by this study, VBP mediates pyroptosis of myeloid cells through the activation of the inflammasome sensor Nlrp1. In addition, we demonstrated that VBP suppresses tumor growth in syngeneic tumor models utilizing cancer cell lines that are responsive to other immunotherapeutics.^[7, 87, 103] It remains to be elucidated if and which inflammasome effector functions are responsible for anti-tumor effects mediated by VBP. Caspase-1 cleaves and activates the proinflammatory cytokines IL-1 β and IL-18.^[48] To determine if either IL-1 β or IL-18 are required for the anti-tumor immune response induced by VBP, knockouts of these cytokines can be included into the tumor model we established in this study. Additionally, mice lacking the IL-18 binding protein (IL-18BP) can be utilized to see if elevated IL-18 serum levels in those mice alter tumor growth in our models. Caspase-1 further activates the pyroptotic death inducing protein GSDMD.^[38, 48] It is possible that the anti-tumor effects of VBP depend on the induction of death in responding cells. Having evidence that VBP induces pyroptotic death in myeloid cells (this study and others)^[10, 105, 112], it will be intriguing to investigate whether death of myeloid cells which promote tumor growth or suppress an immune response is required for VBP's function. Using cell line specific GSDMD knockouts will help to address if this inflammasome effector molecule is required or contributes to the anti-tumor effects.

The second question to expand on our findings will be to define the cellular response activated by VBP. The cellular response to VBP can be divided into two cell populations: 1.) The cells that express caspase-1 and pyroptose as direct response to VBP. 2.) Cells that respond to caspase-1 dependent signals to enhance anti-tumor immunity. To determine the first group, we would conditionally ablate caspase-1 in candidate cell types. Knowing that myeloid cells pyroptose upon VBP treatment (we and others)^[10, 105, 112], floxed caspase-1 mice can be crossed to mice expressing Cre recombinase under a Lysm promotor, specifically depleting caspase-1 in the myeloid compartment. Including those knockout mice into the established tumor models will reveal if VBP induced pyroptosis of myeloid cells is required for its anti-tumor properties. An unbiased approach to determine the first cell population can be to exploit ASC-CFP reporter mice. These mice express a fluorescent ASC adaptor fusion protein (ASC-citrine) that retains the function of endogenous ASC.^[113] By forming fluorescent specks upon exposure to inflammasome activators, both in vitro and in vivo, we will be

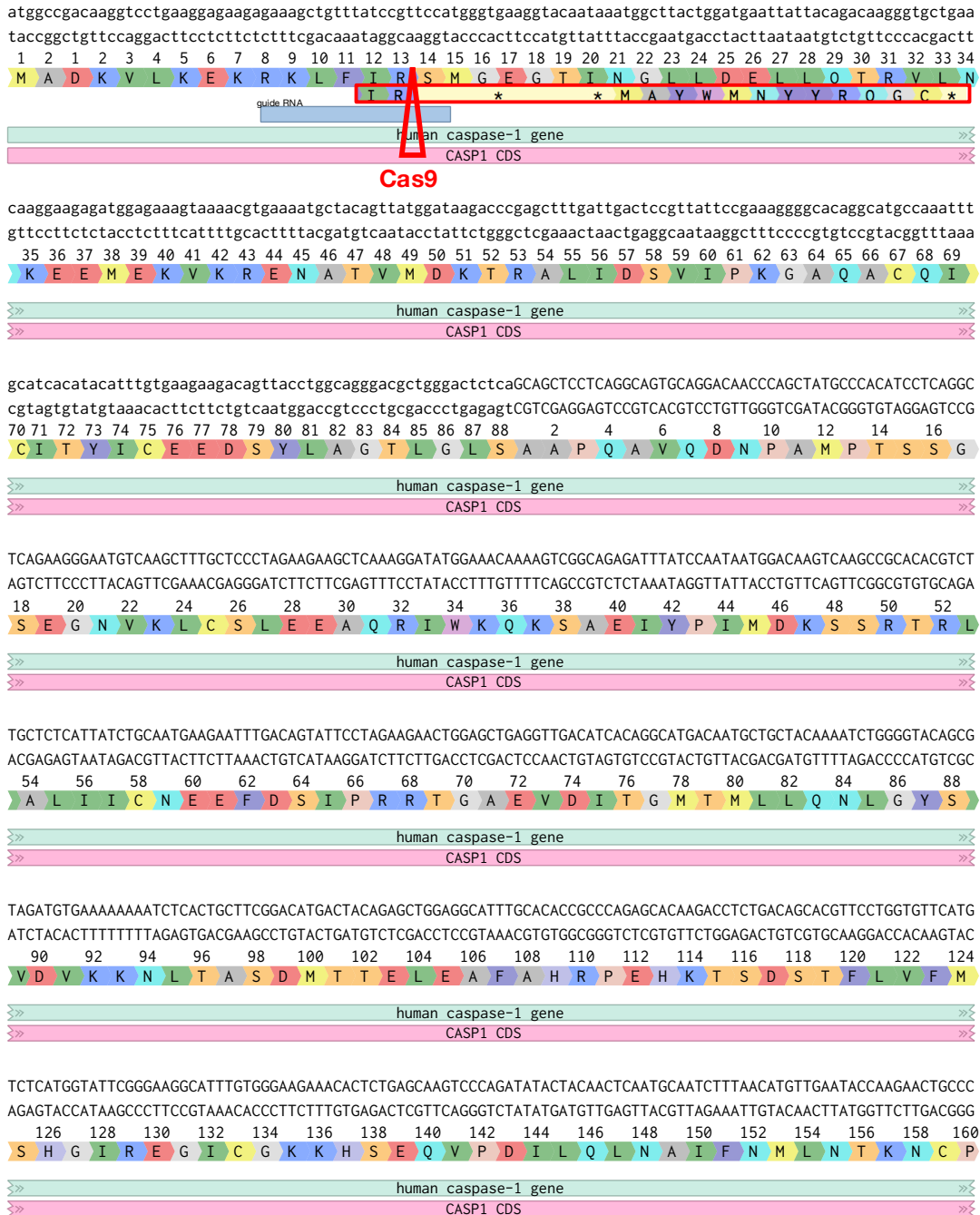
able to detect responding cells in the TME or other tissues by flow cytometry and immunofluorescence. In order to determine the second cell group of interest, we could perform a candidate-approach based on the effectors IL-1 β and IL-18. IL-1 β is a potent chemo attractant of neutrophils^[26, 44]. Therefore, we can investigate differential infiltration of neutrophils into VBP treated tumors or if VBP alters the activation status of neutrophils. IL-18 is known to modulate the adaptive immune response^[45], amongst others by inducing IFN- γ . IFN- γ is known to be important in the YUMMER spontaneous rejection model^[87]. Hence, we could evaluate T-cell infiltration, activation and polarization using flow cytometry in determining whether VBP modulates T-cells. Finally, to determine if VBP functions by depleting different myeloid populations we could further monitor other cell types such as macrophages, monocytes and dendritic cells within the TME. This would likewise be done by monitoring their abundance and activation status using flow cytometry.

Targeting inflammasomes to adjuvant immunotherapies is a promising prospect of future cancer treatment approaches. Given our promising results with the MC38, a thoroughly studied cancer cell line, together with the melanoma cell lines YUMMER1.7-GFP and YUMMER1.7, we are confident that VBP can be applicable to a various set of cancer models. The next step here will be to demonstrate whether the anti-tumor effects on MC38, YUMMER1.7-GFP and YUMMER1.7 tumors depend on Nlrp1 and caspase-1. Therefore, Nlrp1 and caspase-1 knockout mice should be included in future experiments to determine the importance of this inflammasome sensor and the effector molecule in our models. Further attempts should be initiated to broaden the spectrum to investigate other inflammasome sensors in their ability to enhance a tumoricidal immune response. Hereby, we would determine whether Nlrp1 is required or unique in its capability to mediate an anti-tumor response or if targeting other inflammasome sensors will phenocopy the effects we describe in our experiments. Two alternative are Nlrp3 and Nlrc4. For investigating the role of Nlrp3, we would exploit an Nlrp3 gain of function (GOF) allele combined with a tamoxifen inducible Cre recombinase. By specific administration of tamoxifen to the tumor we would be able to determine whether local activated Nlrp3 phenocopies the effects of VBP administration. Ways of regional administration of tamoxifen can be either directed by application on the skin covering the tumor or injection into the tumor. Nlrp3 is of interest because it is considered to be activated by homeostatic alterations of the cell, rather than PAMPs.^[38]

^{42]} This might implicate Nlrp3 as uniquely suitable to pharmacological activation relative to other inflammasome sensors. In parallel it could be assayed whether Nlrc4 is sufficient to enhance an anti-tumor response. Here we could take advantage of a synthetic agonist of Nlrc4, FlaTox. FlaTox is a fusion protein designed by linking the flagelin of *Legionella pneumophila* (FlaA) to the N-terminal domain of B. anthracis lethal factor (LF). Through LF mediated direct delivery into the cytosol by the protective antigen (PA) channel, FlaTox directly activates NAIP5/Nlrp4 without infection.^[114, 115] To test whether local activation of Nlrc4 phenocopies VBP administration, FlaTox can be likewise plied by administration to the skin or injection into the tumors. Using these approaches will help to address the question whether activating inflammasome sensors can be utilized to enhance an anti-tumor response.

These approaches presented, will provide important information to further decipher VBP's anti-tumor properties and significantly broaden the scope of this project to increase the interest of a wider public.

Supplementary Figures



Supplementary Figure 1 Scheme of THP1 CASP1-/- B

List of Figures

FIGURE 1 SIMPLIFIED SCHEMATICS OF POSSIBLE INFLAMMASOME COMPLEX CONTAINING ASC AND CASPASE-1. SCHEME WAS CREATED BY THE AUTHOR OF THIS THESIS AND DESIGNED INSPIRED BY BROZ AND DIXIT^[38] 14

FIGURE 2 STRUCTURE OF VALBORO-PRO. SOURCE: PUBCHEM; URL: [HTTPS://PUBCHEM.NCBI.NLM.NIH.GOV](https://pubchem.ncbi.nlm.nih.gov) 20

FIGURE 3 MOUSE DERIVED PRIMARY MACROPHAGES EXPRESS DPP8 AND DPP9. RNA SEQUENCING OF MBMDMS; UNPUBLISHED DATA GENERATED AND PROVIDED BY THE FLAVELL LAB. 22

FIGURE 4 VBP LEADS TO LDH RELEASE IN WT AND NLR4^{-/-}, BUT NOT CASP1^{-/-} MBMDMS. MBMDMS WERE TREATED WITH 25μM VBP FOR 24 HOURS. STATISTICAL SIGNIFICANCE WAS ASSAYED WITH STUDENT’S T-TEST. **P<0.005 23

FIGURE 5 NLRP1 IS THE RESPONSIVE SENSOR FOR VBP INDUCED PYROPTOSIS IN MBMDMS. MBMDMS WERE GENERATED FROM MICE OF INDICATED GENOTYPES AND TREATED WITH 25μM VBP FOR 24H. LDH LEAKAGE WAS ASSAYED TO ESTIMATE LYTIC CELL DEATH. ****P<0.0005, **P<0.005 36

FIGURE 6 IMMUNOFLUORESCENT STAINING OF ASC AND CASPASE SPECK FORMATION. CELLS WERE SEEDED IN A GLASS BOTTOM 24 WELL AND TREATED WITH 25μM VBP FOR 24 HOURS OR 5 HOURS WITH 100NG/ML LPS PLUS 15 MIN 10μM NIGERICIN, RESPECTIVELY. A) VBP INDUCES ASC AND CASPASE-1 SPECK FORMATION IN WT CELLS. YELLOW FLUORESCENCE INDICATES COLOCALISATION. B) VBP INDUCED ASC SPECK FORMATION IN WT AND CASPASE-1 KNOCKOUTS BUT NOT NLRP1^{-/-}. IMAGES WERE TAKEN AND KINDLY PROVIDED BY JAMES RICHARD BREWER..... 37

FIGURE 7 WESTERN BLOT DETECTION OF CASP-1 AND PRO- IL-1B. MBMDMS WERE STIMULATED FOR 24H WITH 25μM VBP OR 100NG/ML LPS AND 10μM NIGERICIN, RESPECTIVELY. A) DETECTION OF PRO-CASPASE-1 AND P20 CLEAVAGE PRODUCT. B) DETECTION OF IL-1B (PRO-IL-1B AND MATURE IL-1B ARE DISTINGUISHABLE VIA THEIR SIZE). 38

FIGURE 8 VBP DOES NOT ATTENUATE TUMOR GROWTH IN EL4 SYNGENEIC TUMOR MODEL. MICE WERE TREATED TWICE DAILY WITH 20μG VBP, TUMOR VOLUMES WERE ASSAYED WITH A CALIPER, MEASURING 2 DIMENSIONS, SERUM WAS COLLECTED FOR FURTHER ANALYSIS. A) AVERAGE TUMOR GROWTH CURVES (BARS INDICATE SEM). B) TUMOR GROWTH CURVES OF INDIVIDUAL MICE; STATISTICAL SIGNIFICANCE OF DIFFERENCES IN GROWTH CURVES WAS ASSAYED WITH 2-WAY-ANOVA. 39

FIGURE 9 VBP EFFECTS ON CYTOKINE LEVELS IN SERUM. SERUM WAS COLLECTED OF MICE TREATED WITH VEHICLE CONTROL OR VBP FOR 11 DAYS. CYTOKINE LEVELS OF A) IL-18, B) IL-1B AND C) CXCL1 WERE ASSAYED WITH ELISA. STATISTICAL SIGNIFICANCE WAS ASSAYED WITH UNPAIRED T-TEST. **** P< 0.0005. 41

FIGURE 10 VBP ATTENUATES TUMOR GROWTH IN MC38 MODEL. 500K MC38 CELLS WERE INJECTED SUBCUTANEOUSLY. MICE WERE TREATED WITH 20μG VBP OR VEHICLE CONTROL TWICE DAILY P.O. STARTING ON DAY 2 A) AVERAGE OF TUMOR GROWTH CURVES OF WT MICE TREATED WITH VBP OR VEHICLE CONTROL (ERROR BARS INDICATE SEM; SIGNIFICANCE WAS ASSAYED WITH 2-WAY-ANOVA). B) PLOT OF INDIVIDUAL GROWTH CURVES. **P<0.005 42

FIGURE 11 VBP ATTENUATES TUMOR GROWTH IN YUMMER1.7-GFP MODEL. 500K CELLS WERE INJECTED SUBCUTANEOUSLY. MICE WERE TREATED WITH 20μG VBP OR VEHICLE CONTROL TWICE DAILY P.O. STARTING ON DAY2. A) AVERAGE OF TUMOR GROWTH CURVES OF WT MICE TREATED WITH VBP OR VEHICLE CONTROL (ERROR BARS INDICATE SEM; SIGNIFICANCE WAS ASSAYED WITH 2-WAY-ANOVA). B) KAPLAN-MEIER-GRAPH DISPLAYING TUMOR PREVALENCE (RIGHT). *P <0.05 43

FIGURE 12 VBP CAUSES TUMOR REGRESSION IN YUMMER1.7 CANCER MODEL. 500K CELLS WERE INJECTED SUBCUTANEOUSLY. MICE WERE TREATED WITH 20μG VBP OR VEHICLE CONTROL TWICE DAILY P.O. STARTING ON DAY2. A) AVERAGE OF TUMOR GROWTH CURVES OF WT MICE TREATED WITH VBP OR VEHICLE CONTROL (ERROR BARS INDICATE SEM; *P <0.05,

| | |
|---|----|
| SIGNIFICANCE WAS ASSAYED WITH 2-WAY-ANOVA). B) KAPLAN-MEIER-GRAPH DISPLAYING TUMOR PREVALENCE (RIGHT, TUMORS THAT NEVER EXCEEDED A TOTAL VOLUME OF 15MM ³ ARE EXCLUDED OF THE KAPLAN-MEIER-PLOT). | 44 |
| FIGURE 13 VBP DOES NOT DIRECTLY INDUCE PYROPTOSIS IN YUMMER1.7 CELLS. A) LDH RELEASE ASSAY OF VBP RESPONSIVE GFP-THP1 CELLS IN COMPARISON TO YUMMER1.7; CELLS WERE TREATED WITH 100μM VBP FOR 24H. STATISTICAL SIGNIFICANCE WAS ASSAYED WITH STUDENT'S T-TEST. ****p<0.0005 | 44 |
| FIGURE 14 THP1 ASC AND DPP9 KNOCKOUTS. A) WESTERN BLOT OF HETEROGENEOUS ASC AND DPP9 KNOCKOUTS AFTER LENTIVIRUS TRANSDUCTION. B) WESTERN BLOT OF ASC AND DPP9 KNOCKOUT CELL LINES AFTER MONOCLONAL EXPANSION. sgRNA INDICATES GUIDE RNA SEQUENCE USED TO KNOCK OUT GOI..... | 45 |
| FIGURE 15 VALIDATION OF THP1 KNOCKOUTS OF INFLAMMASOME COMPONENTS. A) REPRESENTATIVE IMAGES OF FAILED KNOCKOUT CONFIRMATION OF NLRP1 AND CASP1. B) LDH RELEASE ASSAY OF THP1 INFLAMMASOME KNOCKOUT CLONES COMPARED TO WT THP1. C) SEQUENCE ALIGNMENT OF HUMAN WT CASPASE-1 GENE (NHI REFSEQ CM000673.2) AND SGRNA 2 TARGETED CASP ^{-/-} CLONE B. D) LDH RELEASE ASSAY OF NLRP1 ^{-/-} CLONES. | 47 |
| FIGURE 16 DPP ACTIVITY ASSAY. THP1 CELL LYSATES WERE INCUBATED FOR 2H AT 37°C WITH VEHICLE CONTROL (DMSO) OR VBP. A) MONITORING OF PNA ACCUMULATION OVER THE COURSE OF 2 HOURS. B) REPRESENTATION OF ΔABS/MIN AS A PROXY FOR DPP ACTIVITY. SIGNIFICANCE WAS ASSAYED WITH STUDENT'S T-TEST. **p<0.005. | 49 |
| FIGURE 17 DPPs ARE SENSITIVE TO H ₂ O ₂ CONCENTRATIONS. THP1 CELL LYSATES WERE TREATED WITH INCREASING DOSES OF H ₂ O ₂ TO ASSAY THEIR SENSITIVITY TO ALTERATIONS IN REDOX STATUS. A) MONITORING OF PNA ACCUMULATION OVER THE COURSE OF 2 HOURS. B) DPP ACTIVITY SHOWN AS ΔABS/MIN IN DEPENDENCE OF H ₂ O ₂ CONCENTRATION. | 50 |
| SUPPLEMENTARY FIGURE 1 SCHEME OF THP1 CASP1 ^{-/-} B | 56 |

List of Tables

| | |
|--|----|
| TABLE 1 ELISA KITS FOR CYTOKINE DETECTION | 27 |
| TABLE 2 GUIDERNA SEQUENCES FOR 1-GUIDED CRISPR/CAS9 TARGETING IN THP1 CELLS | 29 |
| TABLE 3 GUIDERNA SEQUENCES FOR 2-GUIDED CRISPR/CAS9 TARGETING OF HUMAN NLRP1 | 30 |
| TABLE 4 ANTIBODIES FOR WESTERN BLOT DETECTION | 33 |

References

1. WorldHealthOrganization. **Cancer (Key Facts)**. In; 2018.
2. Ferlay J, Soerjomataram I, Ervik M, Dikshit R, Eser S, Mathers C, et al. **GLOBOCAN 2012 v1.0, Cancer Incidence and Mortality Worldwide: IARC CancerBase No. 11 [Internet]**. In. Lyon, France: International Agency for Research on Cancer; 2013.
3. Bray F, Ren J-S, Masuyer E, Ferlay J. **Global estimates of cancer prevalence for 27 sites in the adult population in 2008**. *International Journal of Cancer* 2012; 132(5):1133-1145.
4. Farkona S, Diamandis EP, Blasutig IM. **Cancer immunotherapy: the beginning of the end of cancer?** *BMC Medicine* 2016; 14:73.
5. Pardoll DM. **The blockade of immune checkpoints in cancer immunotherapy**. *Nat Rev Cancer* 2012; 12(4):252-264.
6. LaFleur MW, Muroyama Y, Drake CG, Sharpe AH. **Inhibitors of the PD-1 Pathway in Tumor Therapy**. *J Immunol* 2018; 200(2):375-383.
7. Efremova M, Rieder D, Klepsch V, Charoentong P, Finotello F, Hackl H, et al. **Targeting immune checkpoints potentiates immunoediting and changes the dynamics of tumor evolution**. *Nature Communications* 2018; 9:32.
8. Patil S, Rao RS, Majumdar B. **T-cell Exhaustion and Cancer Immunotherapy**. *Journal of International Oral Health : JIOH* 2015; 7(8):i-ii.
9. Adams S, Miller GT, Jesson MI, Watanabe T, Jones B, Wallner BP. **PT-100, a small molecule dipeptidyl peptidase inhibitor, has potent antitumor effects and augments antibody-mediated cytotoxicity via a novel immune mechanism**. *Cancer Res* 2004; 64.
10. Okondo MC, Johnson DC, Sridharan R, Go EB, Chui AJ, Wang MS, et al. **DPP8/9 inhibition induces pro-caspase-1-dependent monocyte and macrophage pyroptosis**. *Nature chemical biology* 2017; 13(1):46-53.
11. Chow MT, Moller A, Smyth MJ. **Inflammation and immune surveillance in cancer**. *Semin Cancer Biol* 2012; 22(1):23-32.
12. Cooper GM. **The Development and Causes of Cancer**. In: *The Cell: A Molecular Approach*, 2 edn. Sunderland (MA): Sinauer Associates; 2000.
13. **World Cancer Report 2014**. In. Edited by BW S, CW W. Lyon: International Agency for Research on Cancer; 2014.
14. Arruebo M, Vilaboa N, Sáez-Gutierrez B, Lambea J, Tres A, Valladares M, et al. **Assessment of the Evolution of Cancer Treatment Therapies**. *Cancers* 2011; 3(3):3279-3330.
15. Floros T, Tarhini AA. **Anticancer Cytokines: Biology and Clinical Effects of IFN- α 2, IL-2, IL-15, IL-21, and IL-12**. *Seminars in oncology* 2015; 42(4):539-548.
16. Goldberg JL, Sondel PM. **Enhancing Cancer Immunotherapy Via Activation of Innate Immunity**. *Seminars in oncology* 2015; 42(4):562-572.
17. Fink PJ. **The Cancer Immunotherapy Revolution: Mechanistic Insights**. *J Immunol* 2018; 200(2):371-372.
18. Grivennikov SI, Greten FR, Karin M. **Immunity, Inflammation, and Cancer**. *Cell* 2010; 140(6):883-899.
19. Hu B, Elinav E, Huber S, Strowig T, Hao L, Hafemann A, et al. **Microbiota-induced activation of epithelial IL-6 signaling links inflammasome-driven inflammation with transmissible cancer**. *Proceedings of the National Academy of Sciences of the United States of America* 2013; 110(24):9862-9867.

20. Dupaul-Chicoine J, Arabzadeh A, Dagenais M, Douglas T, Champagne C, Morizot A, et al. **The Nlrp3 Inflammasome Suppresses Colorectal Cancer Metastatic Growth in the Liver by Promoting Natural Killer Cell Tumoricidal Activity.** *Immunity* 2015; 43(4):751-763.
21. Gonzalez S, González-Rodríguez AP, Suárez-Álvarez B, López-Soto A, Huergo-Zapico L, Lopez-Larrea C. **Conceptual aspects of self and nonself discrimination.** *Self Nonself* 2011; 2(1):19-25.
22. Ribatti D. **The concept of immune surveillance against tumors: The first theories.** *Oncotarget* 2017; 8(4):7175-7180.
23. Swann JB, Smyth MJ. **Immune surveillance of tumors.** *Journal of Clinical Investigation* 2007; 117(5):1137-1146.
24. Wang M, Zhao J, Zhang L, Wei F, Lian Y, Wu Y, et al. **Role of tumor microenvironment in tumorigenesis.** *J Cancer* 2017; 8(5):761-773.
25. Liu Y, Zeng G. **Cancer and Innate Immune System Interactions: Translational Potentials for Cancer Immunotherapy.** *Journal of Immunotherapy (Hagerstown, Md : 1997)* 2012; 35(4):299-308.
26. Nicolas-Avila JA, Adrover JM, Hidalgo A. **Neutrophils in Homeostasis, Immunity, and Cancer.** *Immunity* 2017; 46(1):15-28.
27. Ventola CL. **Cancer Immunotherapy, Part 1: Current Strategies and Agents.** *Pharmacy and Therapeutics* 2017; 42(6):375-383.
28. Rosenberg SA. **IL-2: The First Effective Immunotherapy for Human Cancer.** *The Journal of Immunology* 2014; 192(12):5451.
29. Nozawa H, Chiu C, Hanahan D. **Infiltrating neutrophils mediate the initial angiogenic switch in a mouse model of multistage carcinogenesis.** *Proceedings of the National Academy of Sciences* 2006; 103(33):12493.
30. Bronkhorst IHG, Ly LV, Jordanova ES, Vrolijk J, Versluis M, Luyten GPM, et al. **Detection of M2-Macrophages in Uveal Melanoma and Relation with Survival.** *Investigative Ophthalmology & Visual Science* 2011; 52(2):643-650.
31. Tanaka A, Sakaguchi S. **Regulatory T cells in cancer immunotherapy.** *Cell Research* 2017; 27(1):109-118.
32. Amezcua RA, Kaech SM. **The chronicles of T-cell exhaustion.** *Nature* 2017; 543:190.
33. Yang Y. **Cancer immunotherapy: harnessing the immune system to battle cancer.** *The Journal of Clinical Investigation* 2015; 125(9):3335-3337.
34. Karachaliou N, Gonzalez-Cao M, Sosa A, Berenguer J, Bracht JWP, Ito M, et al. **The combination of checkpoint immunotherapy and targeted therapy in cancer.** *Annals of Translational Medicine* 2017; 5(19):388.
35. Signore A. **About inflammation and infection.** *EJNMMI Res* 2013; 3(1):8.
36. Hu B, Elinav E, Huber S, Booth CJ, Strowig T, Jin C, et al. **Inflammation-induced tumorigenesis in the colon is regulated by caspase-1 and NLRC4.** *Proceedings of the National Academy of Sciences of the United States of America* 2010; 107(50):21635-21640.
37. Chaplin DD. **Overview of the Immune Response.** *The Journal of allergy and clinical immunology* 2010; 125(2 Suppl 2):S3-23.
38. Broz P, Dixit VM. **Inflammasomes: mechanism of assembly, regulation and signalling.** *Nat Rev Immunol* 2016; 16(7):407-420.
39. Guo H, Callaway JB, Ting JP. **Inflammasomes: mechanism of action, role in disease, and therapeutics.** *Nat Med* 2015; 21(7):677-687.
40. Liston A, Masters SL. **Homeostasis-altering molecular processes as mechanisms of inflammasome activation.** *Nat Rev Immunol* 2017; 17(3):208-214.

41. Tang D, Kang R, Coyne CB, Zeh HJ, Lotze MT. **PAMPs and DAMPs: signal 0s that spur autophagy and immunity.** *Immunol Rev* 2012; 249(1):158-175.
42. Martinon F, Burns K, Tschopp J. **The Inflammasome: A Molecular Platform Triggering Activation of Inflammatory Caspases and Processing of proIL- β .** *Molecular Cell* 2002; 10(2):417-426.
43. Man SM, Karki R, Kanneganti T-D. **Molecular mechanisms and functions of pyroptosis, inflammatory caspases and inflammasomes in infectious diseases.** *Immunological reviews* 2017; 277(1):61-75.
44. Soehnlein O, Steffens S, Hidalgo A, Weber C. **Neutrophils as protagonists and targets in chronic inflammation.** *Nature Reviews Immunology* 2017; 17:248.
45. Kaplanski G. **Interleukin-18: Biological properties and role in disease pathogenesis.** *Immunol Rev* 2018; 281(1):138-153.
46. Masters SL, Gerlic M, Metcalf D, Preston S, Pellegrini M, O'Donnell JA, et al. **NLRP1 inflammasome activation induces pyroptosis of hematopoietic progenitor cells.** *Immunity* 2012; 37(6):1009-1023.
47. Man SM, Kanneganti T-D. **Regulation of inflammasome activation.** *Immunological reviews* 2015; 265(1):6-21.
48. Broz P, von Moltke J, Jones JW, Vance RE, Monack DM. **Differential requirement for Caspase-1 autoproteolysis in pathogen-induced cell death and cytokine processing.** *Cell host & microbe* 2010; 8(6):471-483.
49. Bryan NB, Dorfleutner A, Rojanasakul Y, Stehlik C. **Activation of inflammasomes requires intracellular redistribution of the apoptotic speck-like protein containing a caspase recruitment domain.** *J Immunol* 2009; 182(5):3173-3182.
50. Guey B, Bodnar M, Manié SN, Tardivel A, Petrilli V. **Caspase-1 autoproteolysis is differentially required for NLRP1b and NLRP3 inflammasome function.** *Proceedings of the National Academy of Sciences of the United States of America* 2014; 111(48):17254-17259.
51. Yu CH, Moecking J, Geyer M, Masters SL. **Mechanisms of NLRP1-Mediated Autoinflammatory Disease in Humans and Mice.** *J Mol Biol* 2017.
52. Chavarria-Smith J, Mitchell PS, Ho AM, Daugherty MD, Vance RE. **Functional and Evolutionary Analyses Identify Proteolysis as a General Mechanism for NLRP1 Inflammasome Activation.** *PLoS Pathog* 2016; 12(12):e1006052.
53. Joseph CS, E. VR. **The NLRP1 inflammasomes.** *Immunological Reviews* 2015; 265(1):22-34.
54. Finger JN, Lich JD, Dare LC, Cook MN, Brown KK, Duraiswami C, et al. **Autolytic proteolysis within the function to find domain (FIIND) is required for NLRP1 inflammasome activity.** *J Biol Chem* 2012; 287(30):25030-25037.
55. Van Opendenbosch N, Gurung P, Vande Walle L, Fossoul A, Kanneganti T-D, Lamkanfi M. **Activation of the NLRP1b inflammasome independently of ASC-mediated caspase-1 autoproteolysis and speck formation.** *Nature Communications* 2014; 5:3209.
56. Hellmich KA, Levinsohn JL, Fattah R, Newman ZL, Maier N, Sastalla I, et al. **Anthrax lethal factor cleaves mouse nlrp1b in both toxin-sensitive and toxin-resistant macrophages.** *PLoS One* 2012; 7(11):e49741.
57. Ewald SE, Chavarria-Smith J, Boothroyd JC. **NLRP1 Is an Inflammasome Sensor for Toxoplasma gondii.** *Infection and Immunity* 2014; 82(1):460-468.
58. Zhong FL, Mamai O, Sborgi L, Boussofara L, Hopkins R, Robinson K, et al. **Germline NLRP1 Mutations Cause Skin Inflammatory and Cancer Susceptibility Syndromes via Inflammasome Activation.** *Cell* 2016; 167(1):187-202 e117.

59. Ridker PM, Everett BM, Thuren T, MacFadyen JG, Chang WH, Ballantyne C, et al. **Antiinflammatory Therapy with Canakinumab for Atherosclerotic Disease.** *N Engl J Med* 2017; 377(12):1119-1131.
60. Ridker PM, MacFadyen JG, Thuren T, Everett BM, Libby P, Glynn RJ, et al. **Effect of interleukin-1 β inhibition with canakinumab on incident lung cancer in patients with atherosclerosis: exploratory results from a randomised, double-blind, placebo-controlled trial.** *The Lancet* 2017; 390(10105):1833-1842.
61. McDonald JK. **An overview of protease specificity and catalytic mechanisms: aspects related to nomenclature and classification.** *Histochemical Journal* 1985; 17:773-785.
62. Waumans Y, Baerts L, Kehoe K, Lambeir AM, De Meester I. **The Dipeptidyl Peptidase Family, Prolyl Oligopeptidase, and Prolyl Carboxypeptidase in the Immune System and Inflammatory Disease, Including Atherosclerosis.** *Front Immunol* 2015; 6:387.
63. Koivisto V. **Discovery of dipeptidyl-peptidase IV--a 40 year journey from bench to patient.** *Diabetologia* 2008; 51(6):1088-1089.
64. Ghorpade DS, Ozcan L, Zheng Z, Nicoloso SM, Shen Y, Chen E, et al. **Hepatocyte-secreted DPP4 in obesity promotes adipose inflammation and insulin resistance.** *Nature* 2018; 555(7698):673-677.
65. Barnett A. **DPP-4 inhibitors and their potential role in the management of type 2 diabetes.** *Int J Clin Pract* 2006; 60(11):1454-1470.
66. Tinoco AD, Tagore DM, Saghatelian A. **Expanding the dipeptidyl peptidase 4-regulated peptidome via an optimized peptidomics platform.** *J Am Chem Soc* 2010; 132(11):3819-3830.
67. Juillerat-Jeanneret L, Tafelmeyer P, Golshayan D. **Fibroblast activation protein-alpha in fibrogenic disorders and cancer: more than a prolyl-specific peptidase?** *Expert Opin Ther Targets* 2017; 21(10):977-991.
68. Wagner L, Klemann C, Stephan M, von Horsten S. **Unravelling the immunological roles of dipeptidyl peptidase 4 (DPP4) activity and/or structure homologue (DASH) proteins.** *Clin Exp Immunol* 2016; 184(3):265-283.
69. Chen W-T, Kelly T, Ghersi G. **DPPIV, seprase, and related serine peptidases in multiple cellular functions.** In: *Current Topics in Developmental Biology*: Academic Press; 2003. pp. 207-232.
70. Rosenblum JS, Kozarich JW. **Prolyl peptidases: a serine protease subfamily with high potential for drug discovery.** *Curr Opin Chem Biol* 2003; 7.
71. Jiang G-M, Xu W, Du J, Zhang K-S, Zhang Q-G, Wang X-W, et al. **The application of the fibroblast activation protein α -targeted immunotherapy strategy.** *Oncotarget* 2016; 7(22):33472-33482.
72. Wilson CH, Zhang HE, Gorrell MD, Abbott CA. **Dipeptidyl peptidase 9 substrates and their discovery: current progress and the application of mass spectrometry-based approaches.** *Biol Chem* 2016; 397(9):837-856.
73. Zhang H, Maqsudi S, Rainczuk A, Duffield N, Lawrence J, Keane FM, et al. **Identification of novel dipeptidyl peptidase 9 substrates by two-dimensional differential in-gel electrophoresis.** *FEBS J* 2015; 282(19):3737-3757.
74. Ross B, Krapp S, Augustin M, Kierfersauer R, Arciniega M, Geiss-Friedlander R, et al. **Structures and mechanism of dipeptidyl peptidases 8 and 9, important players in cellular homeostasis and cancer.** *Proc Natl Acad Sci U S A* 2018; 115(7):E1437-E1445.
75. Park J, M. Knott H, Nadvi N, Collyer C, Wang X, Church W, et al. **Reversible Inactivation of Human Dipeptidyl Peptidases 8 and 9 by Oxidation.** 2008.

76. Geiss-Friedlander R, Parmentier N, Moller U, Urlaub H, Van den Eynde BJ, Melchior F. **The cytoplasmic peptidase DPP9 is rate-limiting for degradation of proline-containing peptides.** *J Biol Chem* 2009; 284(40):27211-27219.
77. Gall MG, Chen Y, Vieira de Ribeiro AJ, Zhang H, Bailey CG, Spielman DS, et al. **Targeted Inactivation of Dipeptidyl Peptidase 9 Enzymatic Activity Causes Mouse Neonate Lethality.** *PLOS ONE* 2013; 8(11):e78378.
78. Kim M, Minoux M, Piaia A, Kueng B, Gapp B, Weber D, et al. **DPP9 enzyme activity controls survival of mouse migratory tongue muscle progenitors and its absence leads to neonatal lethality due to suckling defect.** *Developmental Biology* 2017; 431(2):297-308.
79. Barreira da Silva R, Laird ME, Yatim N, Fiette L, Ingersoll MA, Albert ML. **Dipeptidylpeptidase 4 inhibition enhances lymphocyte trafficking, improving both naturally occurring tumor immunity and immunotherapy.** *Nat Immunol* 2015; 16(8):850-858.
80. Walsh MP, Duncan B, Larabee S, Krauss A, Davis JPE, Cui Y, et al. **Val-BoroPro Accelerates T Cell Priming via Modulation of Dendritic Cell Trafficking Resulting in Complete Regression of Established Murine Tumors.** *PLOS ONE* 2013; 8(3):e58860.
81. Coutts SJ, Kelly TA, Snow RJ, Kennedy CA, Barton RW, Adams J, et al. **Structure-activity relationships of boronic acid inhibitors of dipeptidyl peptidase IV. 1. Variation of the P2 position of Xaa-boroPro dipeptides.** *J Med Chem* 1996; 39.
82. Adams S, Miller GT, Jesson MI, Watanabe T, Jones B, Wallner BP. **PT-100, a Small Molecule Dipeptidyl Peptidase Inhibitor, Has Potent Antitumor Effects and Augments Antibody-Mediated Cytotoxicity via a Novel Immune Mechanism.** *Cancer Research* 2004; 64(15):5471.
83. Pelegrin P, Barroso-Gutierrez C, Surprenant A. **P2X₇ Receptor Differentially Couples to Distinct Release Pathways for IL-1 β in Mouse Macrophage.** *The Journal of Immunology* 2008; 180(11):7147.
84. Kovarova M, Hesker PR, Jania L, Nguyen M, Snouwaert JN, Xiang Z, et al. **NLRP1-dependent pyroptosis leads to acute lung injury and morbidity in mice.** *J Immunol* 2012; 189(4):2006-2016.
85. Case CL, Kohler LJ, Lima JB, Strowig T, de Zoete MR, Flavell RA, et al. **Caspase-11 stimulates rapid flagellin-independent pyroptosis in response to *Legionella pneumophila*.** *Proceedings of the National Academy of Sciences* 2013; 110(5):1851.
86. Sutterwala FS, Ogura Y, Szczepanik M, Lara-Tejero M, Lichtenberger GS, Grant EP, et al. **Critical Role for NALP3/CIAS1/Cryopyrin in Innate and Adaptive Immunity through Its Regulation of Caspase-1.** *Immunity* 2006; 24(3):317-327.
87. Wang J, Perry CJ, Meeth K, Thakral D, Damsky W, Micevic G, et al. **UV-induced somatic mutations elicit a functional T cell response in the YUMMER1.7 Mouse Melanoma Model.** *Pigment cell & melanoma research* 2017; 30(4):428-435.
88. Sanjana NE, Shalem O, Zhang F. **Improved vectors and genome-wide libraries for CRISPR screening.** *Nature methods* 2014; 11(8):783-784.
89. Campeau E, Ruhl VE, Rodier F, Smith CL, Rahmberg BL, Fuss JO, et al. **A Versatile Viral System for Expression and Depletion of Proteins in Mammalian Cells.** *PLoS ONE* 2009; 4(8):e6529.
90. Chan FK-M, Moriwaki K, De Rosa MJ. **Detection of Necrosis by Release of Lactate Dehydrogenase (LDH) Activity.** *Methods in molecular biology (Clifton, NJ)* 2013; 979:65-70.
91. DiPeso L, Ji DX, Vance RE, Price JV. **Cell death and cell lysis are separable events during pyroptosis.** *Cell Death Discovery* 2017; 3:17070.
92. Dinarello CA. **Interleukin-1 in the pathogenesis and treatment of inflammatory diseases.** *Blood* 2011; 117(14):3720-3732.

93. Sawant KV, Poluri KM, Dutta AK, Sepuru KM, Troshkina A, Garofalo RP, et al. **Chemokine CXCL1 mediated neutrophil recruitment: Role of glycosaminoglycan interactions.** *Scientific Reports* 2016; 6:33123.
94. Eruslanov EB, Bhojnagarwala PS, Quatromoni JG, Stephen TL, Ranganathan A, Deshpande C, et al. **Tumor-associated neutrophils stimulate T cell responses in early-stage human lung cancer.** *The Journal of Clinical Investigation* 2014; 124(12):5466-5480.
95. Suttman H, Riemensberger J, Bentien G, Schmaltz D, Stöckle M, Jocham D, et al. **Neutrophil Granulocytes Are Required for Effective & Bacillus Calmette-Guérin; Immunotherapy of Bladder Cancer and Orchestrate Local Immune Responses.** *Cancer Research* 2006; 66(16):8250.
96. Peiro C, Lorenzo O, Carraro R, Sanchez-Ferrer CF. **IL-1 β Inhibition in Cardiovascular Complications Associated to Diabetes Mellitus.** *Front Pharmacol* 2017; 8:363.
97. Attur MG, Dave M, Cicolletta C, Kang P, Goldring MB, Patel IR, et al. **Reversal of Autocrine and Paracrine Effects of Interleukin 1 (IL-1) in Human Arthritis by Type II IL-1 Decoy Receptor: POTENTIAL FOR PHARMACOLOGICAL INTERVENTION.** *Journal of Biological Chemistry* 2000; 275(51):40307-40315.
98. Li L, Fei Z, Ren J, Sun R, Liu Z, Sheng Z, et al. **Functional imaging of interleukin 1 beta expression in inflammatory process using bioluminescence imaging in transgenic mice.** *BMC Immunology* 2008; 9(1):49.
99. Reilly KM. **The Effects of Genetic Background of Mouse Models of Cancer: Friend or Foe?** *Cold Spring Harbor Protocols* 2016; 2016(3):pdb.top076273.
100. Puccini J, Dorstyn L, Kumar S. **Genetic background and tumour susceptibility in mouse models.** *Cell Death and Differentiation* 2013; 20(7):964-964.
101. Eager RM, Cunningham CC, Senzer NN, Stephenson J, Anthony SP, O'Day SJ, et al. **Phase II assessment of talabostat and cisplatin in second-line stage IV melanoma.** *BMC Cancer* 2009; 9(1):263.
102. Eager RM, Cunningham CC, Senzer N, Richards DA, Raju RN, Jones B, et al. **Phase II Trial of Talabostat and Docetaxel in Advanced Non-small Cell Lung Cancer.** *Clinical Oncology* 2009; 21(6):464-472.
103. Meeth K, Wang J, Micevic G, Damsky W, Bosenberg MW. **The YUMM lines: a series of congenic mouse melanoma cell lines with defined genetic alterations.** *Pigment cell & melanoma research* 2016; 29(5):590-597.
104. Wang H, Yang H, Shivalila CS, Dawlaty MM, Cheng AW, Zhang F, et al. **One-Step Generation of Mice Carrying Mutations in Multiple Genes by CRISPR/Cas-Mediated Genome Engineering.** *Cell* 2013; 153(4):910-918.
105. Johnson DC, Taabazuing CY, Okondo MC, Chui AJ, Rao SD, Brown FC, et al. **DPP8/DPP9 inhibitor-induced pyroptosis for treatment of acute myeloid leukemia.** *Nature Medicine* 2018; 24(8):1151-1156.
106. Rummey C, Metz G. **Homology models of dipeptidyl peptidases 8 and 9 with a focus on loop predictions near the active site.** *Proteins* 2007; 66(1):160-171.
107. Liu Y, Patricelli MP, Cravatt BF. **Activity-based protein profiling: The serine hydrolases.** *Proceedings of the National Academy of Sciences of the United States of America* 1999; 96(26):14694-14699.
108. Ray PD, Huang B-W, Tsuji Y. **Reactive oxygen species (ROS) homeostasis and redox regulation in cellular signaling.** *Cellular signalling* 2012; 24(5):981-990.
109. Sasse AD, Sasse EC, Clark LG, Ulloa L, Clark OA. **Chemoimmunotherapy versus chemotherapy for metastatic malignant melanoma.** *Cochrane Database Syst Rev* 2007; 1.

110. Hu B, Elinav E, Flavell RA. **Inflammasome-mediated suppression of inflammation-induced colorectal cancer progression is mediated by direct regulation of epithelial cell proliferation.** *Cell Cycle* 2011; 10(12):1936-1939.
111. Guo B, Fu S, Zhang J, Liu B, Li Z. **Targeting inflammasome/IL-1 pathways for cancer immunotherapy.** *Sci Rep* 2016; 6:36107.
112. Taabazuing CY, Okondo MC, Bachovchin DA. **Pyroptosis and Apoptosis Pathways Engage in Bidirectional Crosstalk in Monocytes and Macrophages.** *Cell Chem Biol* 2017; 24(4):507-514 e504.
113. Tzeng T-CJ, Schattgen S, Monks B, Wang D, Cerny A, Latz E, et al. **A fluorescent reporter mouse for inflammasome assembly demonstrates an important role for cell bound and free ASC specks during in vivo infection.** *Cell reports* 2016; 16(2):571-582.
114. Lei-Leston AC, Murphy AG, Maloy KJ. **Epithelial Cell Inflammasomes in Intestinal Immunity and Inflammation.** *Frontiers in Immunology* 2017; 8(1168).
115. Moltke JH. **Suicidal Cells and Lipid Storms: Mechanisms and Consequences of Cytokine-independent Inflammasome Activation:** UC Berkeley; 2012.